

17. Oiso N, Fukai K, Ishii M. Interleukin 4 receptor alpha chain polymorphism Gln551Arg is associated with adult atopic dermatitis in Japan. *Br J Dermatol.* 2000;142:1003-1006.
18. Rosa-Rosa L, Zimmermann N, Bernstein JA, Rothenberg ME, Khurana Hershey GK. The R576 IL-4 receptor alpha allele correlates with asthma severity. *J Allergy Clin Immunol.* 1999;104:1008-1014.
19. Arima K, Umeshita-Suyama R, Sakata Y, et al. Upregulation of IL-13 concentration in vivo by the IL13 variant associated with bronchial asthma. *J Allergy Clin Immunol.* 2002;109:980-987.
20. Correia O, Delgado L, Ramos JP, Resende C, Torrinha JA. Cutaneous T-cell recruitment in toxic epidermal necrolysis: further evidence of CD8⁺ lymphocyte involvement. *Arch Dermatol.* 1993;129:466-468.
21. Miyauchi H, Hosokawa H, Akaeda T, Iba H, Asada Y. T-cell subsets in drug-induced toxic epidermal necrolysis: possible pathogenic mechanism induced by CD8-positive T cells. *Arch Dermatol.* 1991;127:851-855.
22. Del Prete G. Human Th1 and Th2 lymphocytes: their role in the pathophysiology of atopy. *Allergy.* 1992;47:450-455.



Human conjunctival epithelial cells express functional Toll-like receptor 5

K Kojima, M Ueta, J Hamuro, Y Hozono, S Kawasaki, N Yokoi and S Kinoshita

Br. J. Ophthalmol. 2008;92;411-416; originally published online 22 Jan 2008;
doi:10.1136/bjo.2007.128322

Updated information and services can be found at:

<http://bjo.bmj.com/cgi/content/full/92/3/411>

These include:

Data supplement

"web only appendices"

<http://bjo.bmj.com/cgi/content/full/bjo.2007.128322/DC1>

References

This article cites 37 articles, 16 of which can be accessed free at:

<http://bjo.bmj.com/cgi/content/full/92/3/411#BIBL>

1 online articles that cite this article can be accessed at:

<http://bjo.bmj.com/cgi/content/full/92/3/411#otherarticles>

Rapid responses

You can respond to this article at:

<http://bjo.bmj.com/cgi/eletter-submit/92/3/411>

**Email alerting
service**

Receive free email alerts when new articles cite this article - sign up in the box at the top right corner of the article

Notes

To order reprints of this article go to:

<http://journals.bmj.com/cgi/reprintform>

To subscribe to *British Journal of Ophthalmology* go to:

<http://journals.bmj.com/subscriptions/>

Human conjunctival epithelial cells express functional Toll-like receptor 5

K Kojima, M Ueta, J Hamuro, Y Hozono, S Kawasaki, N Yokoi, S Kinoshita

► Additional supplemental figures 1 and 2 are published online only at <http://bjo.bmj.com/content/vol92/issue3>

Department of Ophthalmology, Kyoto Prefectural University of Medicine, Kyoto, Japan

Correspondence to: M Ueta, Department of Ophthalmology, Kyoto Prefectural University of Medicine, Kajii-cho 465, Hirokoji-agaru, Kawaramachi-dori, Kamigyo-ku, Kyoto 602-0841, Japan; mueta@ophth.kpu-m.ac.jp

Accepted 25 November 2007
Published Online First
22 January 2008

ABSTRACT

Purpose: The expression and function of Toll-like receptor 5 (TLR5) was analysed in human conjunctival epithelial cells (HCjEC).

Methods: The expression of TLR5 in HCjEC was studied by reverse transcriptase (RT) PCR and flow cytometry. The amount of interleukin (IL) 6 and IL-8 proteins was determined by ELISA. Messenger RNA expression elicited by stimulation with flagellins derived from *Pseudomonas aeruginosa*, *Serratia marcescens*, *Salmonella typhimurium*, and *Bacillus subtilis* was assayed by quantitative RT-PCR. The localisation of TLR5 protein in human conjunctival epithelium was detected immunohistochemically.

Results: HCjEC expressed TLR5-specific mRNA and TLR5 protein. In HCjEC stimulated with flagellins derived from *P aeruginosa* and *S marcescens*, IL-6 and IL-8 production was increased and IL-6 and IL-8 mRNA was upregulated. Flagellins from *S typhimurium* and *B subtilis* did not induce the upregulation of these genes and proteins. TLR5 protein was detected on the basolateral but not the apical side of human conjunctival epithelium.

Conclusions: Human conjunctival epithelium harbours functional TLR5. Considering the spatially selective basolateral localisation of TLR5 protein, it was postulated that flagellins from ocular pathogenic bacteria induce inflammatory responses when disruption of the epithelial barrier permits their transmigration to the basolateral side but not under healthy physiological conditions on the ocular surface.

The ocular surface consists of mucosal epithelium composed of corneal and conjunctival epithelial cells. As are other mucosal epithelia, the ocular mucosal epithelium is continuously challenged by pathogenic and non-pathogenic microbes. The mucosal epithelium is thought to represent a first line of defence against diverse microbes, not only by providing a physical barrier, but also by producing pro-inflammatory cytokines and antimicrobial peptides.¹ Ocular surface epithelium such as corneal and conjunctival epithelium produce antimicrobial peptides similar to other mucosal epithelium.²⁻⁵

Toll-like receptors (TLR), pattern recognition receptors that sense conserved pathogen-associated molecular patterns, are the key receptors for the recognition of microbes.^{4,5} TLR were initially shown to be expressed and functional in immunocompetent cells such as macrophages and dendritic cells (DC); subsequently, their expression in a variety of cells including intestinal and airway epithelial cells was documented.^{6,7} Signalling through TLR induces the activation of transcription factors for antimicrobial genes and cytokines.⁸ TLR5 recognises bacterial flagellin,⁹ a component

protein of bacterial flagella. Flagella are present in both Gram-positive and Gram-negative bacteria; they are essential for bacterial motility, invasion, and chemotaxis. *Pseudomonas aeruginosa* and *Serratia marcescens* are the bacteria associated with ocular surface with flagella.¹⁰⁻¹¹

We previously reported that human corneal epithelial cells (HCEC) express TLR2 and TLR4 intracellularly but not on their cell surface, and that HCEC do not secrete interleukin (IL) 6 or IL-8 in response to peptidoglycan and lipopolysaccharide stimulation. This defective response may contribute to the immunosilent environment in the epithelium for commensal bacteria inhabiting the ocular surface.¹² We documented that TLR3 on poly I : C-treated HCEC responded by producing pro-inflammatory cytokines and interferon β .¹³ Others¹⁴⁻¹⁶ reported that functional TLR in HCEC play a pivotal role in innate immunity to pathogen-associated molecular patterns. Elucidation of the unique innate immune responses of HCEC that are distinct from those of immune-competent cells will lead to a better understanding of the host-commensal symbiosis on the ocular surface.

P aeruginosa flagellin elicits the inflammatory responses of HCEC in a TLR5-dependent manner.¹⁷ We reported that HCEC express TLR5 and secrete pro-inflammatory cytokines in response to flagellin derived from ocular bacteria that are pathogenic, but not to non-pathogenic ocular bacteria.¹⁸ We found that flagellin derived from *S. typhimurium*, a bacterium pathogenic in the intestine but not on the ocular surface, evoked a response by human intestinal epithelial cells but not HCEC.¹⁸

Whereas the critical homeostatic role of TLR in corneal epithelium has been discussed extensively in the literature, there are few reports on the role of TLR in conjunctival epithelium. Cook *et al*¹⁹ and Bonini *et al*²⁰ documented the expression of TLR2, TLR4, and TLR9 in human conjunctival epithelial cells (HCjEC). The expression and function of TLR5 in conjunctival epithelium has not, however, been clarified yet.

In this study we confirmed the expression and function of TLR5 in HCjEC. We document that flagellins derived from *P aeruginosa* and *S marcescens* can trigger the innate immune response in HCjEC expressing TLR5, and TLR5 was selectively expressed on the basolateral but not the apical side of conjunctival epithelium.

MATERIALS AND METHODS

Human conjunctival epithelial cells

This study was approved by the institutional review board of Kyoto Prefectural University of Medicine, in Kyoto, Japan. All experimental

procedures were conducted in accordance with the principles set forth in the Helsinki Declaration. The purpose of the research and the experimental protocol were explained to all patients and their informed consent was obtained.

For reverse transcriptase (RT) PCR, we obtained HCjEC from healthy volunteers by brush cytology. A tiny brush (Cytobrush S; Medscand AM, Malmo, Sweden) was used to scrape epithelial cells from the bulbar conjunctiva. For ELISA, real-time quantitative PCR, and flow cytometric analysis, we harvested primary HCjEC from conjunctival tissue obtained at conjunctivochalasis surgery.²¹ The cells were cultured using a modification of previously described methods.²² Briefly, conjunctival tissues were washed and immersed for 1 h at 37°C in 1.2 U ml⁻¹ purified dispase (Roche Diagnostic Ltd, Basel, Switzerland). Epithelial cells were detached, collected, and cultured in low-calcium k-SFM medium supplemented with 0.2 ng ml⁻¹ human recombinant epidermal growth factor (Invitrogen, Carlsbad, California, USA), 25 mg ml⁻¹ bovine pituitary extract (Invitrogen), and 1% antibiotic-antimycotic solution. Cell colonies usually became obvious within three or four days. After reaching 80% confluence in seven to 10 days, the cells were seeded and after their subconfluence, they were used in subsequent procedures.

Bacterial flagellins used in this study

Flagellins derived from *P aeruginosa* and *S marcescens* were obtained from Inotek Pharmaceuticals (Beverly, Massachusetts, USA); flagellins from *Salmonella typhimurium* and *Bacillus subtilis* were from InvivoGen (San Diego, California, USA). *S typhimurium* flagellin is a strong pathogen that gains entrance into intestinal mucosa by penetrating enterocytes;²³ it does not penetrate to the ocular surface mucosa. The pathogen *S marcescens* is implicated in approximately 5–10% of Gram-negative corneal ulcers related to contact lens wear.^{10–11} The pathogenic potential of *B subtilis* is reportedly weak or absent.²⁴ *P aeruginosa* is an opportunistic ocular pathogen that can initiate a highly destructive corneal infection in humans^{10–11} and is involved in up to 70% of contact lens-related bacterial keratitis cases.²⁵

Purification of mononuclear cells from peripheral blood

The procedures were described elsewhere.¹³ Briefly, we obtained peripheral venous blood samples from volunteers who had given their previous informed consent. Mononuclear cells isolated in lymphoprep tubes (Daiichi Pure Chemicals, Tokyo, Japan) were stimulated for 24 h with the different flagellins.

Reverse transcriptase PCR

We analysed HCjEC for TLR1–10 RNA expression as described in our previous study.¹³ Briefly, total RNA was isolated from HCjEC and human peripheral mononuclear cells using Trizol Reagent (Life Technologies, New York, New York, USA) according to the manufacturer's instructions. For the RT reaction we used the SuperScript Preamplification Kit (Invitrogen). PCR amplification was with DNA polymerase (cTaq; Toyobo, Japan); the conditions were 38 cycles at 94°C for one minute, annealing for one minute, and 72°C for one minute on a commercial PCR machine (GeneAmp; Perkin-Elmer Applied Biosystems, Foster City, California, USA). The primers were as described in our previous study (table 1).¹⁵ RNA integrity was assessed electrophoretically in ethidium bromide-stained 1.5% agarose gels.

Enzyme-linked immunosorbent assay

Primary HCjEC were examined to quantify cytokine secretion as described in our previous report.¹⁸ Briefly, primary HCjEC were plated in 24-well plates and after reaching subconfluence were either left untreated or incubated for 24 h with each flagellin at a final concentration of 100 ng/ml or with 10 ng/ml human IL-1 α (R&D Systems, Inc, Minneapolis, Minnesota, USA). The amount of IL-6 and IL-8 secreted in response to flagellin exposure increased with the flagellin concentration; we used 100 ng/ml. As early as 24 h, we found high levels of IL-6 and IL-8 in supernatants from flagellin-exposed cultures of primary HCjEC. IL-6 and IL-8 release into culture supernatants was quantitated using the Opteia IL-6 and IL-8 set (BD Pharmingen, San Diego, California, USA) according to the manufacturer's instructions.

Table 1 The primer list of Toll-like receptor (TLR)

| Gene (accession no) | Primer sense antisense | Product size | Annealing |
|---------------------|---|--------------|-----------|
| TLR1 (NM003263) | 5'-TGCCCTGCCTATATGCAA-3' 5'-GAACACATCGCTGACAACT-3' | 555 bp | 54 |
| TLR2 (XM003304) | 5'-GCCAAAGTCTTGATTGATTGG-3' 5'-TTGAAGTTCTCCAGCTCCTG-3' | 346 bp | 52 |
| TLR3 (NM003265) | 5'-CGCCAACCTCACAAAGTA-3' 5'-GGAAGCCAAGCAAAGGAA-3' | 689 bp | 54 |
| TLR4 (XM005336) | 5'-TGGATACGTTTCTTATAAG-3' 5'-GAAATGGAGGCACCCCTTC-3' | 506 bp | 52 |
| TLR5 (NM003268) | 5'-ATCTGACTGCATTAAGGGGAC-3' 5'-TTGAGCAAAGCATTCTGCAC-3' | 567 bp | 52 |
| TLR6 (NM006068) | 5'-CCTCAACCACATAGAAACGAC-3' 5'-CACCACTATACTCTCAACCCAA-3' | 531 bp | 50 |
| TLR7 (NM016562) | 5'-AGTGTCTAAAGAACCTGG-3' 5'-CCTGGCCTTACAGAAATG-3' | 544 bp | 50 |
| TLR8 (NM016610) | 5'-CAGAAATAGCAGGCGTAACACATCA-3' 5'-AATGTCACAGGTGCATTCAAAGGG-3' | 639 bp | 56 |
| TLR9 (NM017442) | 5'-GTGCCCACTTCTCCATG-3' 5'-GGCACAGTCATGATGTTGTTG-3' | 259 bp | 50 |
| TLR10 (NM030956) | 5'-CTTTGATCTGCCCTGGTATCTC-3' 5'-AGCCACACATTTACGCCTATCCT-3' | 497 bp | 52 |
| GAPDH (XM033263) | 5'-CCATCACCATCTTCCAGGAG-3' 5'-CCTGCTTACCACCTTCTTG-3' | 575 bp | 60 |

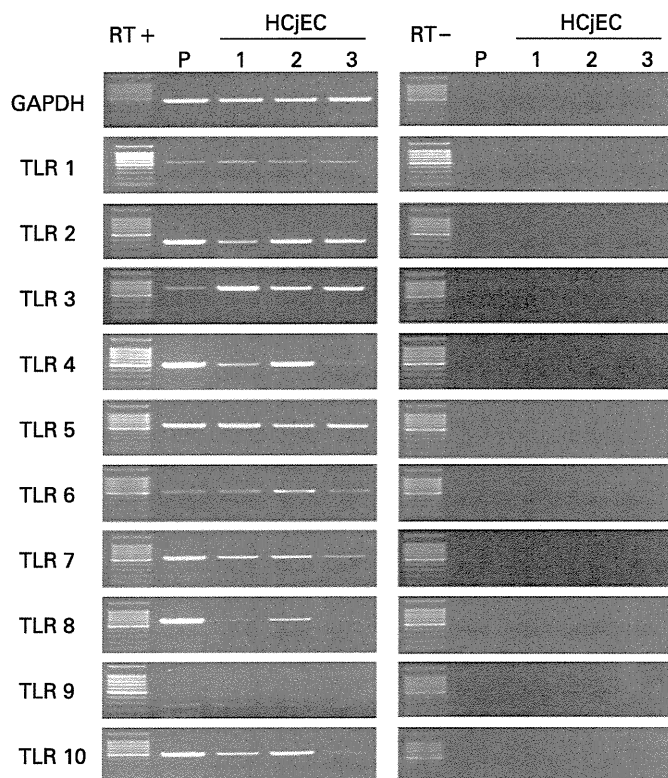


Figure 1 Human conjunctival epithelial cells (HCjEC) express Toll-like receptor (TLR) 1–10-specific mRNA. Total RNA was isolated from human conjunctival epithelial cells. For the reverse transcriptase (RT) reaction, we used the SuperScript preamplification system. PCR amplification was with DNA polymerase; primers are listed in table 1. Human mononuclear cells were the positive control (P).

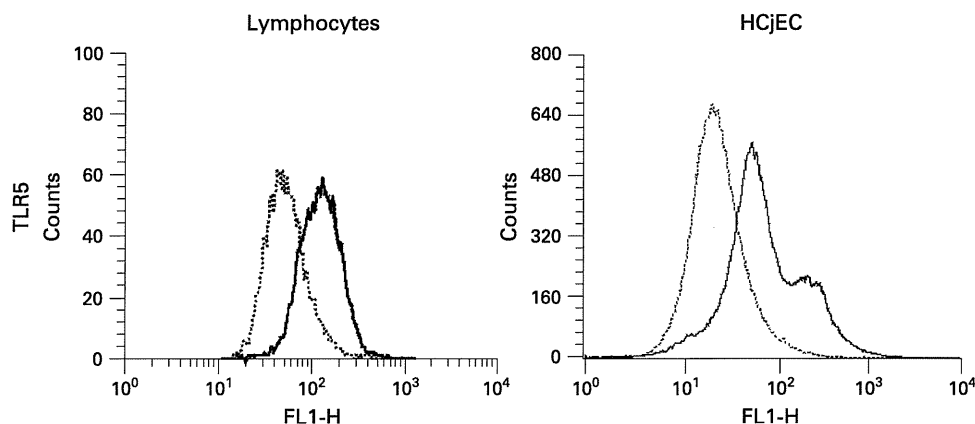
Flow cytometric analysis

HCjEC were analysed for TLR5 expression by flow cytometry as previously described.^{11–18} We purchased mouse anti-human TLR5 monoclonal antibody from Abcam (Cambridge, UK); it recognises an intracellular epitope in the cytoplasmic domain of TLR5.

Immunohistochemical study of TLR5 in human conjunctival sections

Serial sections of human conjunctiva were prepared from samples obtained at conjunctivochalasis surgery. These were fixed for 30 minutes with methanol, incubated overnight in a moist chamber at 4°C with mouse anti-human TLR5

Figure 2 Human conjunctival epithelial cells (HCjEC) express Toll-like receptor (TLR) 5 protein. Intracellular fluorescence-activated cell sorter analysis showed that TLR5 is expressed in HCjEC. As the TLR5 antibody recognises the intracellular domain of the TLR5 complex, we performed intracellular staining. Lymphocytes were the positive control. Histogram data are representative of three separate experiments (solid line, TLR5 antibody; dotted line, isotype control).



monoclonal antibody (Abcam) or isotype control mouse IgG2a (DakoCytomation, Kyoto, Japan), and washed in phosphate buffered saline. Alexa Fluor 488 goat anti-mouse IgG (H+L) (Molecular Probes, Eugene, Oregon, USA) was applied for 1 h at room temperature, the slides were washed and then antifade mounting medium with propidium iodide was applied (Vectashield; Vector Laboratories, Burlingame, California, USA).

Real-time quantitative PCR

Real-time quantitative PCR was performed on an ABI-prism 7700 (Applied Biosystems) according to previously described procedures.^{13–18} The initial amount of RNA used for reverse transcribing to complementary DNA was approximately 1 µg and the cDNA was used at the original concentration for quantitative PCR. The stimulation time used in this study (1 h) was optimal for the maximum induction of IL-6 and IL-8 mRNA expressions (see supplemental fig 2 published online only).

The primers and probes for human IL-6 (Hs00174131), IL-8 (Hs00174103) and human GAPDH (Hs 4326317E) were from Perkin-Elmer Applied Biosystems. Quantitative PCR was used to measure the expression of IL-6 and IL-8 mRNA in HCjEC treated for 1 h with flagellin derived from four different microbial bacteria (100 ng/ml) or human IL-α. The quantification data were normalised to the expression of the housekeeping gene GAPDH.

Data analysis

Data were expressed as the mean ± SE and evaluated by Student's t-test using the Excel program.

RESULTS

TLR-specific mRNA and TLR5 protein expression in HCjEC

TLR1–10-specific mRNA expression was present in HCjEC harvested by impression cytology from healthy volunteers; TLR5-specific mRNA was expressed at levels comparable to mononuclear cells (fig 1). This finding demonstrates that the TLR5 gene is constitutively expressed in HCjEC. The TLR5 protein was also expressed by primary HCjEC harvested from conjunctival tissue at levels comparable to lymphocytes (fig 2).

Primary HCjEC respond only to flagellin derived from ocular pathogenic bacteria

To assess whether the flagellins used were able to induce an inflammatory response in immunocompetent cells, we stimulated fractionated human peripheral mononuclear cells for 24 h

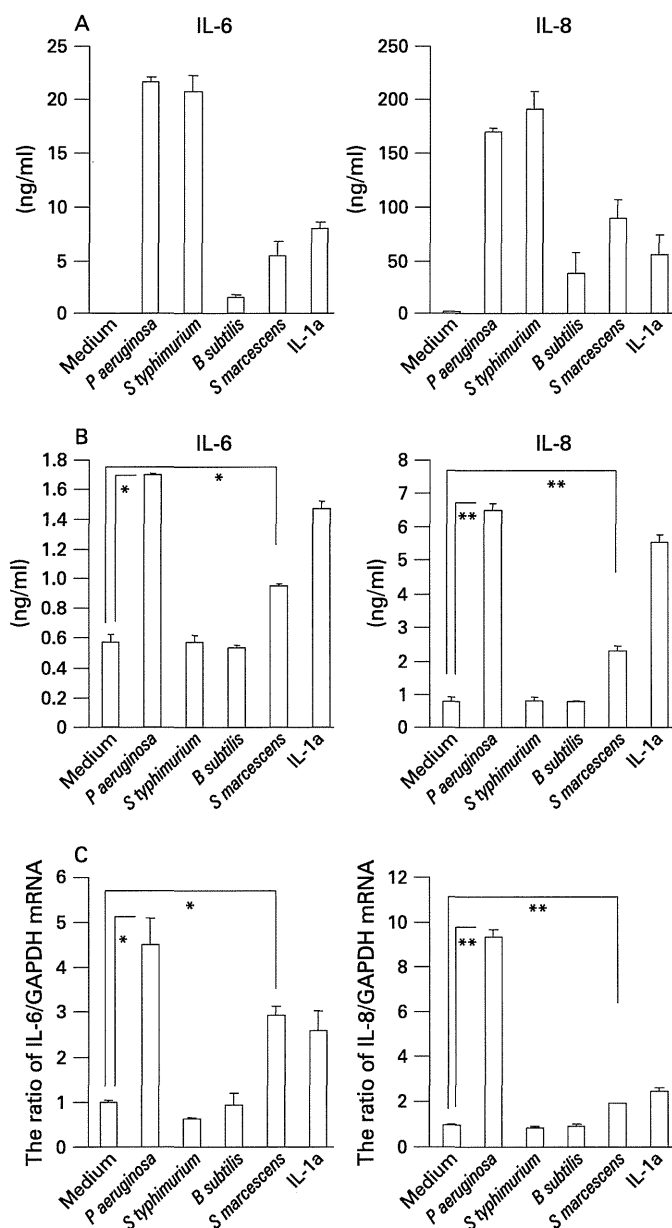


Figure 3 Production and mRNA expression of IL-6 and IL-8 in human conjunctival epithelial cells exposed to various flagellins. (A) To determine whether the flagellins induce an inflammatory response, fractionated human peripheral mononuclear cells were stimulated for 24 h with *P. aeruginosa*, *S. typhimurium*, *B. subtilis*, or *S. marcescens*-derived flagellin at a concentration of 100 ng/ml. The supernatants were harvested and the concentration of IL-6 and IL-8 was measured. (B) To quantify inflammatory cytokine secretion, human conjunctival epithelial cells (HCjEC) were plated in 24-well plates. Upon reaching subconfluence they were left untreated or exposed for 24 h to flagellins derived from the four different microbial bacteria (100 ng/ml) or 10 ng/ml human IL-1a. The supernatants were harvested to measure IL-6 and IL-8 concentrations. (C) Quantitative reverse transcriptase PCR was used to measure the expression of IL-6 and IL-8 mRNA in HCjEC treated for 1 h with flagellin derived from four different microbial bacteria (100 ng/ml) or 10 ng/ml human IL-1a. The quantification data were normalised to the expression of the housekeeping gene GAPDH. The Y axis shows the increase of specific mRNA over unstimulated samples. Data show the representative results from two independent experiments (A) or three independent experiments (B, C). Data represent mean \pm SEM from the representative experiments with triplicated dishes (* <0.05 , ** <0.005).

with *P. aeruginosa*, *S. typhimurium*, *B. subtilis* or *S. marcescens*-derived flagellin. All flagellins induced the production of significant levels of the inflammatory cytokines IL-6, and IL-8 (fig 3A).

Our results indicated that the flagellins derived from the four distinct microbes were able to induce pro-inflammatory cytokine production by human mononuclear cells. As we previously documented that HCjEC produced IL-6 and IL-8 in response to flagellins derived from ocular pathogenic, but not non-pathogenic, bacteria,¹⁸ we investigated whether HCjEC exhibited a similar response. We found that in primary HCjEC, flagellins derived from *P. aeruginosa* and *S. marcescens*, but not those derived from *S. typhimurium* and *B. subtilis* elicited a significant increase in the secretion of IL-6 and IL-8 protein (fig 3B). The mRNA expression levels specific for IL-6 and IL-8 were considerably elevated in primary HCjEC stimulated with *P. aeruginosa* and *S. marcescens*-derived flagellin. In contrast, neither IL-6 nor IL-8-specific mRNA levels were significantly elevated in primary HCjEC stimulated with *S. typhimurium* and *B. subtilis*-derived flagellin (fig 3C). These results suggest that, like HCjEC, primary HCjEC respond to ocular pathogenic but not to ocular non-pathogenic flagellins.

We decided on the dose for ELISA and real-time quantitative PCR according to our dose analysis and the recommended concentration of flagellin written in the manufacturer's instructions. As per the manufacturer's instructions, the recommended concentration to achieve TLR5 stimulation is 0.1–100 ng/ml, and the strongest response was achieved with 100 ng/ml *P. aeruginosa* and *S. marcescens*-derived flagellin (see supplemental fig 1 published online only).

TLR5 is expressed basolaterally in conjunctival epithelium

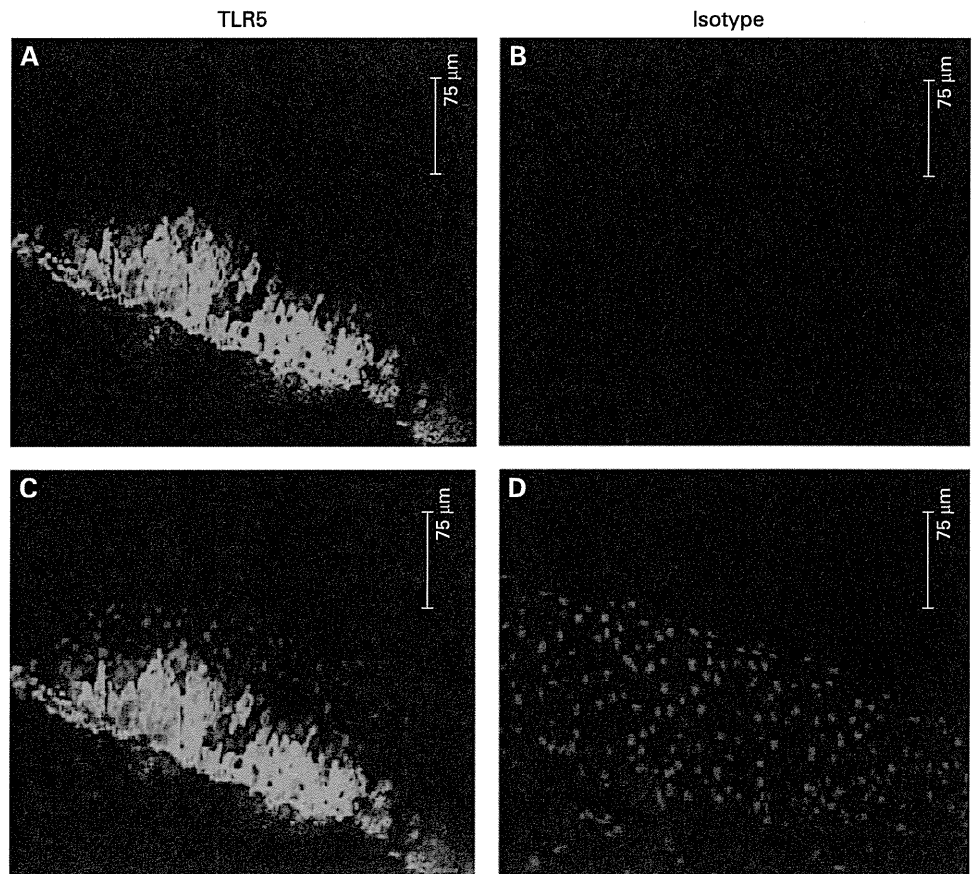
We subjected conjunctival tissues obtained at conjunctivochalasis surgery to immunohistochemical study to determine the presence and localisation of TLR5 expression in stratified conjunctival epithelium. TLR5 protein was consistently and abundantly expressed in human conjunctival epithelium. It was detected only at basal and wing sites, indicating its spatially selective presence on the basolateral but not the apical side (fig 4).

DISCUSSION

This is the report of the expression and function of TLR5 on HCjEC. HCjEC stimulated with flagellins derived from *P. aeruginosa* and *S. marcescens* but not from *S. typhimurium* and *B. subtilis* induced the elevated production and mRNA upregulation of IL-6 and IL-8. TLR5 was selectively expressed on the basolateral but not the apical side.

The ability to detect microbes is an important task of the immune system. Exaggerated host defence reactions of the epithelium to endogenous bacterial flora may start and perpetuate inflammatory mucosal responses.²⁶ Among ocular surface-related bacteria, only a few common causative ocular pathogens, ie *P. aeruginosa* and *S. marcescens*, have flagella; *Staphylococcus epidermidis* and *Pseudomonas acnes*, commensal ocular bacteria,^{27 28} do not. Most, if not all, of the responses to bacterial flagellin are thought to be mediated by TLR5.²⁹ *S. typhimurium* flagellin, strongly pathogenic and pro-inflammatory to intestinal epithelial cells,²³ had little effect on HCjEC. Although *B. subtilis* is one of the related species of *Bacillus cereus*, which is a major cause of severe keratitis, endophthalmitis, and

Figure 4 Localisation of Toll-like receptor (TLR) 5 in a human conjunctival epithelium. TLR5 was detected by immunofluorescence staining. Frozen cryostat sections of a human conjunctiva were incubated with anti-TLR5 antibody (A, C). Isotype control incubation was the negative control (B, D). Bound antibodies were visualised by Alexa Fluor 488 goat anti-mouse IgG, nuclei by propidium iodide (PI) staining. Merged staining of TLR5 and PI shows no TLR5 staining associated with the apical layer of the epithelium.



panophthalmitis,³⁰ *B subtilis* flagellin elicited no immune response in HCjEC. This suggests that TLR5 in HCjEC may discriminate specifically between bacteria that are ocular pathogenic and non-pathogenic.

Whereas *P aeruginosa* and *S marcescens* are common pathogens in keratitis,^{10 11} they do not usually cause conjunctivitis. Conjunctivitis attributable to these bacteria tends to be seen primarily in neonates and immunocompromised hosts.^{31 32} The lamina propria, abundant in immunocompetent cells and lymphatic organs, is located beneath the conjunctival epithelium.³³ On the other hand, the avascular stroma under the corneal epithelium harbours few immunocompetent cells. The host defence in the conjunctival and corneal component may be different and this may account for the difference in the pathogens that result in keratitis and conjunctivitis.

Immunohistochemical data presented here and elsewhere¹⁸ indicate that TLR5 is basolaterally expressed in both conjunctival and corneal epithelium. Similarly, TLR5 is expressed on the basolateral surface of intestinal epithelium and detects invasive flagellated bacteria.²⁹ TLR5 in ocular surface epithelium may be crucial for the sensing of invasive flagellated bacteria. It is possible that the flagellins of *P aeruginosa* and *S marcescens* induce an inflammatory reaction only if the integrity of the epithelial barrier is breached, thereby allowing their transepithelial transport to the basolateral site.

Interestingly, the ocular surface epithelium did not respond to flagellin derived from the enteropathogenic, ocular non-pathogenic bacterium *S typhimurium*. Murine intestinal lamina propria cells can differentiate between pathogenic and non-pathogenic bacteria.³⁴ It remains unknown, however, how TLR can distinguish between pathogenic and non-pathogenic microbes. A

collaboration between co-receptors and TLR may be a possible explanation; a receptor called fimbriae cooperates with TLR4 to distinguish between pathogenic and non-pathogenic bacteria in the urinary tract.³⁵ Alternatively, there may be some minor molecular differences at the site of recognition in TLR5 expressed on different cell types. Mouse and human TLR5 discriminates between different flagellins, and the recognition site on TLR5 has been mapped to the diversified extracellular domain.³⁶ Studies are underway in our laboratory to identify the molecular mechanisms that allow HCjEC to discriminate between flagellins derived from ocular pathogenic and non-pathogenic bacteria.

Another group recently reported that primary HCjEC express TLR5 and respond to *S typhimurium*-derived flagellin.³⁷ Their result differs from the result obtained in our study. The cause of the difference is not evident but it might be due to the dose of flagellin used. That group used an extremely large amount of flagellin in their experiment. Our study confirmed that a much smaller amount (100 ng/ml) of *S typhimurium*-derived flagellin could upregulate IL-8 production in human colonic carcinoma cell line HT29¹⁸ but not HCjEC, and that the same amount of *P aeruginosa*-derived flagellin could also significantly upregulate IL-6 and IL-8 production in HCjEC.

We document that HCjEC possesses functional TLR5, and that conjunctival epithelial cells respond to exposure to flagellins derived from ocular pathogenic but not non-pathogenic bacteria by secreting pro-inflammatory cytokines. Considering the spatially selective localisation of TLR5 protein on the basolateral side of human conjunctival epithelium, an inflammatory reaction may be induced only when flagellin from ocular pathogenic bacteria cross the conjunctival epithelium to the basolateral side.

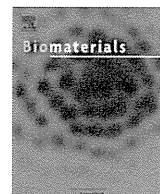
Acknowledgements: The authors would like to thank Ms C Mochida for her technical assistance.

Funding: Supported in part by grants-in-aid for scientific research from the Japanese Ministry of Health, Labour and Welfare, the Japanese Ministry of Education, Culture, Sports, Science and Technology, CREST from JST, a research grant from the Kyoto Foundation for the Promotion of Medical Science and the Intramural Research Fund of Kyoto Prefectural University of Medicine.

Competing interests: None.

REFERENCES

1. **Savkovic SD**, Koutsouris A, Hecht G. Activation of NF-kappaB in intestinal epithelial cells by enteropathogenic *Escherichia coli*. *Am J Physiol* 1997;**273**:C1160–7.
2. **McIntosh RS**, Cade JE, Al-Abed M, et al. The spectrum of antimicrobial peptide expression at the ocular surface. *Invest Ophthalmol Vis Sci* 2005;**46**:1379–85.
3. **Haynes RJ**, Tighe PJ, Dua HS. Antimicrobial defensin peptides of the human ocular surface. *Br J Ophthalmol* 1999;**83**:737–41.
4. **Medzhitov R**, Preston-Hurlburt P, Janeway CA Jr. A human homologue of the *Drosophila* Toll protein signals activation of adaptive immunity. *Nature* 1997;**388**:394–7.
5. **Takeda K**, Kaisho T, Akira S. Toll-like receptors. *Annu Rev Immunol* 2003;**21**:335–76.
6. **Abreu MT**, Vora P, Faure E, et al. Decreased expression of Toll-like receptor-4 and MD-2 correlates with intestinal epithelial cell protection against dysregulated proinflammatory gene expression in response to bacterial lipopolysaccharide. *J Immunol* 2001;**167**:1609–16.
7. **Becker MN**, Diamond G, Verghese MW, et al. CD14-dependent lipopolysaccharide-induced beta-defensin-2 expression in human tracheobronchial epithelium. *J Biol Chem* 2000;**275**:29731–6.
8. **Medzhitov R**, Janeway C Jr. Innate immune recognition: mechanisms and pathways. *Immunity* 2000;**13**:99–109.
9. **Hayashi F**, Smith KD, Ozinsky A, et al. The innate immune response to bacterial flagellin is mediated by Toll-like receptor 5. *Nature* 2001;**410**:1099–103.
10. **Schaefer F**, Bruttin O, Zografos L, et al. Bacterial keratitis: a prospective clinical and microbiological study. *Br J Ophthalmol* 2001;**85**:842–7.
11. **Mayo MS**, Schlitzer RL, Ward MA, et al. Association of *Pseudomonas* and *Serratia* corneal ulcers with use of contaminated solutions. *J Clin Microbiol* 1987;**25**:1398–400.
12. **Ueta M**, Nochi T, Jang MH, et al. Intracellularly expressed TLR2s and TLR4s contribute to an immunosilent environment at the ocular mucosal epithelium. *J Immunol* 2004;**173**:3337–47.
13. **Ueta M**, Hamuro J, Kiyono H, et al. Triggering of TLR3 by poly(I : C) in human corneal epithelial cells to induce inflammatory cytokines. *Biochem Biophys Res Commun* 2005;**331**:285–94.
14. **Zhang J**, Wu XY, Yu FS. Inflammatory responses of corneal epithelial cells to *Pseudomonas aeruginosa* infection. *Curr Eye Res* 2005;**30**:527–34.
15. **Kumar A**, Zhang J, Yu FS. Toll-like receptor 3 agonist poly(I : C)-induced antiviral response in human corneal epithelial cells. *Immunology* 2006;**117**:11–21.
16. **Johnson AC**, Heinzel FP, Diaconu E, et al. Activation of toll-like receptor (TLR)2, TLR4, and TLR9 in the mammalian cornea induces MyD88-dependent corneal inflammation. *Invest Ophthalmol Vis Sci* 2005;**46**:589–95.
17. **Zhang J**, Xu K, Ambati B, et al. Toll-like receptor 5-mediated corneal epithelial inflammatory responses to *Pseudomonas aeruginosa* flagellin. *Invest Ophthalmol Vis Sci* 2003;**44**:4247–54.
18. **Hozono Y**, Ueta M, Hamuro J, et al. Human corneal epithelial cells respond to ocular-pathogenic, but not to nonpathogenic-flagellin. *Biochem Biophys Res Commun* 2006;**347**:238–47.
19. **Cook EB**, Stahl JL, Esnault S, et al. Toll-like receptor 2 expression on human conjunctival epithelial cells: a pathway for *Staphylococcus aureus* involvement in chronic ocular proinflammatory responses. *Ann Allergy Asthma Immunol* 2005;**94**:486–97.
20. **Bonini S**, Micera A, Iovieno A, et al. Expression of Toll-like receptors in healthy and allergic conjunctiva. *Ophthalmology* 2005;**112**:1528–35.
21. **Yokoi N**, Komuro A, Sugita J, et al. Surgical reconstruction of the tear meniscus at the lower lid margin for treatment of conjunctivochalasis. *Adv Exp Med Biol* 2002;**506**:1263–8.
22. **Hirai N**, Kawasaki S, Tanioka H, et al. Pathological keratinisation in the conjunctival epithelium of Sjogren's syndrome. *Exp Eye Res* 2006;**82**:371–8.
23. **Jung HC**, Eckmann L, Yang SK, et al. A distinct array of proinflammatory cytokines is expressed in human colon epithelial cells in response to bacterial invasion. *J Clin Invest* 1995;**95**:55–65.
24. **Oggioni MR**, Pozzi G, Valensini PE, et al. Recurrent septicemia in an immunocompromised patient due to probiotic strains of *Bacillus subtilis*. *J Clin Microbiol* 1998;**36**:325–6.
25. **Mah-Sadorra JH**, Yavuz SG, Najjar DM, et al. Trends in contact lens-related corneal ulcers. *Cornea* 2005;**24**:51–8.
26. **Boehme KW**, Compton T. Innate sensing of viruses by toll-like receptors. *J Virol* 2004;**78**:7867–73.
27. **Ueta M**, Iida T, Sakamoto M, et al. Polyclonality of *Staphylococcus epidermidis* residing on the healthy ocular surface. *J Med Microbiol* 2007;**56**:77–82.
28. **Doyle A**, Beigi B, Early A, et al. Adherence of bacteria to intraocular lenses: a prospective study. *Br J Ophthalmol* 1995;**79**:347–9.
29. **Gewirtz AT**, Navas TA, Lyons S, et al. Cutting edge: bacterial flagellin activates basolaterally expressed TLR5 to induce epithelial proinflammatory gene expression. *J Immunol* 2001;**167**:1882–5.
30. **Drobniewski FA**. *Bacillus cereus* and related species. *Clin Microbiol Rev* 1993;**6**:324–38.
31. **van Ogtrop ML**, van Zoeren-Grobben D, Verbakel-Salmons EM, et al. *Serratia marcescens* infections in neonatal departments: description of an outbreak and review of the literature. *J Hosp Infect* 1997;**36**:95–103.
32. **Shah SS**, Gloor P, Gallagher PG. Bacteremia, meningitis, and brain abscesses in a hospitalized infant: complications of *Pseudomonas aeruginosa* conjunctivitis. *J Perinatol* 1999;**19**:462–5.
33. **Chodosh J**, Kennedy RC. The conjunctival lymphoid follicle in mucosal immunology. *DNA Cell Biol* 2002;**21**:421–33.
34. **Uematsu S**, Jang MH, Chevrier N, et al. Detection of pathogenic intestinal bacteria by Toll-like receptor 5 on intestinal CD11c+ lamina propria cells. *Nat Immunol* 2006;**7**:868–74.
35. **Fischer H**, Yamamoto M, Akira S, et al. Mechanism of pathogen-specific TLR4 activation in the mucosa: fimbriae, recognition receptors and adaptor protein selection. *Eur J Immunol* 2006;**36**:267–77.
36. **Andersen-Nissen E**, Smith KD, Bonneau R, et al. A conserved surface on Toll-like receptor 5 recognizes bacterial flagellin. *J Exp Med* 2007;**204**:393–403.
37. **Li J**, Shen J, Beuerman RW. Expression of toll-like receptors in human limbal and conjunctival epithelial cells. *Mol Vis* 2007;**13**:813–22.



The use of trehalose-treated freeze-dried amniotic membrane for ocular surface reconstruction

Takahiro Nakamura^{a,b,*}, Eiichi Sekiyama^a, Maho Takaoka^a, Adam J. Bentley^c, Norihiko Yokoi^a, Nigel J. Fullwood^c, Shigeru Kinoshita^a

^a Department of Ophthalmology, Kyoto Prefectural University of Medicine, Graduate School of Medicine, 465 Kawaramachi Hirokoji, Kamigyo-ku, Kyoto 602-0841, Japan

^b Research Center for Regenerative Medicine, Doshisha University, Karasuma-Imadegawa, Kamigyo-ku, Kyoto 602-8580, Japan

^c Biomedical Sciences, Lancaster University, Lancaster LA1 4YQ, UK

ARTICLE INFO

Article history:

Received 19 March 2008

Accepted 20 May 2008

Available online 10 June 2008

Keywords:

Trehalose

Amniotic membrane

Freeze-dry

Ocular surface reconstruction

Biocompatibility

ABSTRACT

The aim of this study was to evaluate the efficacy and safety of trehalose-treated freeze-dried amniotic membrane (TT-FDAM) for ocular surface reconstruction. Human AM deprived of amniotic epithelial cells was first incubated with 10% trehalose solution, and then freeze-dried, vacuum-packed, and sterilized with gamma-irradiation. The resultant newly developed TT-FDAM was characterized for its physical, biological, and morphological properties by comprehensive physical assays, immunohistochemistry, electron microscopy, cell adhesion assay, 3D cell culture, and an *in vivo* biocompatibility test. The adaptability of TT-FDAM was markedly improved as compared to FDAM. Immunohistochemistry for several extracellular matrix molecules revealed that the process of freeze-drying and irradiation apparently did not affect its biological properties, however, electron microscopy revealed that the detailed morphological appearance of TT-FDAM is more similar to that of native AM than to FDAM. Intracorneal and scleral-surface transplantation of TT-FDAM showed excellent biocompatibility with ocular surface tissues. Thus, TT-FDAM retained most of the physical, biological, and morphological characteristics of native AM, consequently it is a useful biomaterial for ocular surface reconstruction.

© 2008 Published by Elsevier Ltd.

1. Introduction

The amniotic membrane (AM), whose function is to protect the embryo and to surround and contain the amniotic fluid, has been used as surgical biomaterial in a variety of clinical applications [1,2]. It has been shown to possess various kinds of biological effects such as an anti-inflammatory effect [3,4], anti-fibroblastic activity [5], anti-microbial [6] and anti-angiogenic [7] properties, very limited immunogenicity [8], and a proper substrate for cells. Recently, particular attention has been focused on the AM in the ophthalmologic field, since its variety of characteristics make it ideally suited for use in ocular surface reconstruction. However, some serious biological and logistical problems still remained, such as the deficiency of appropriate sterilization and difficulties in transport and storage.

Recently, we have resolved such serious problems by developing a sterilized, freeze-dried amniotic membrane (FDAM) using a special vacuum-packaging process and gamma-irradiation, and have

successfully developed and adapted it for clinical application [9,10]. Even though FDAM retained most of the biological characteristics of native AM, the manufacturing process (especially the freeze-drying process) ultimately affects some of the characteristics of the AM; therefore it is not completely identical to native AM both physically and biologically [9–11]. Therefore, further improvement of the physical, biological, and morphological characteristics of FDAM is needed in order to adapt it to a wider variety of clinical applications.

Trehalose is a nonreducing disaccharide (C₁₂H₂₂O₁₁) found in high concentrations in a wide variety of organisms that are capable of surviving almost complete dehydration. It is thought to be a storage sugar in the cells, and evidence is accumulating that trehalose production may be a universal stress response. Its presence confers desiccation resistance to bacterial and human cells [12]. Its remarkable effectiveness is clearly due to its ability to replace some of the water in the cell, thereby stabilizing and protecting the cellular membrane and proteins during the freezing process [13]. These findings led us to the interesting hypothesis that trehalose might protect AM from damage during the freeze-drying process and consequently improve the biological quality of FDAM.

In this report, we present the efficacy and safety of trehalose-treated freeze-dried amniotic membrane (TT-FDAM) for ocular surface reconstruction.

* Corresponding author. Department of Ophthalmology, Kyoto Prefectural University of Medicine, Graduate School of Medicine, 465 Kawaramachi Hirokoji, Kamigyo-ku, Kyoto 602-0841, Japan. Tel.: +81 75 251 5578; fax: +81 75 251 5663.
E-mail address: tnakamur@ophth.kpu-m.ac.jp (T. Nakamura).

2. Materials and methods

2.1. Preparation of TT-FDAM

Human AM was prepared following our previously reported standard method [14]. Briefly, after obtaining proper informed consent in accordance with the tenets of the Declaration of Helsinki and with approval by the Institutional Review Board of Kyoto Prefectural University of Medicine, human AMs were obtained at the time of elective cesarean section from volunteers who were seronegative donors. Under sterile conditions, the AM was washed with sterile phosphate buffered saline (PBS) containing antibiotics and antimycotics and cut into pieces measuring approximately 5 × 5 cm. The AM was then deprived of amniotic epithelial cells by incubation with 0.02% ethylene diamine tetraacetic acid (EDTA; Nacalai Tesqu Co., Kyoto, Japan) at 37 °C for 2 h. To protect the structure of denuded AM from damage during the freeze-drying process, denuded AM was further incubated with 10% trehalose solution (TREHA, Hayashibara, Okayama, Japan) at 37 °C for 2 h. This trehalose solution was attentively pre-treated with an ultrasonic machine to remove the micro-bubbles. After that, TT-FDAM was fixed and stretched in the plastic holder to prevent it from crinkling. It was then freeze-dried under vacuum conditions using vacuum freeze-drying apparatuses (TAITEC, Saitama, Japan) for 1 h and then vacuum-packed at room temperature (RT) as soon as possible. Finally, gamma-irradiation (20 kGy) was used to sterilize the resultant TT-FDAM. The manufacturing process of FDAM [9] is almost the same as that of TT-FDAM except for the pre-treatment of the trehalose solution.

2.2. Physical examination of TT-FDAM

To investigate the physical characteristics of TT-FDAM, we examined its thickness, haze, tensile strength, and adaptability. Samples examined in this study were AM without epithelium, FDAM, and TT-FDAM ($N = 5$).

The thickness of each sample (measuring 25 × 25 mm each) was measured by a surface-scanning laser confocal displacement meter (LT-9010M; Keyence, Osaka, Japan). Haze was measured by a turbidimeter (NDH2000, Nippon Denshoku, Tokyo, Japan). Briefly, each 25 × 25 mm sample under the wet condition was placed and fixed on the measuring holder without folds or bubbles. Use of the turbidimeter allowed for the calculation of total light transmittance, diffused transmittance, and parallel transmittance. Haze was calculated as follows: haze = diffused transmittance/total light transmittance. Tensile strength was examined by stretch-stress (SS) tests performed on 10 × 30 mm samples using our previous protocol [9]. Briefly, both ends of each 10 × 30 mm sample under the wet condition were held with a clip. Each sample was then pulled vertically with a uniaxial stretching device. Cross-head speed was set at 10 mm/min. Adaptability was examined by putting the samples on the rabbit corneal surface under the wet condition and calculating the number of AM folds on the cornea under a microscope by three different individuals.

2.3. Immunohistochemistry

Immunohistochemical examinations in this study were carried out using our previously described method [15,16]. Briefly, semi-thin (7 μm) cryostat sections were obtained from unfixed tissue embedded in Tissue-Tek OCT compound (Miles Inc., Elkhart, IN, USA). After fixation with cold acetone for 10 min, the sections were incubated with 1% bovine serum albumin for 30 min. Subsequently, the sections were incubated at RT for 1 h with the primary antibody (Table 1), then washed three times in PBS containing 0.15% TritonX-100 (PBST) for 10 min. The controls consisted of replacing the primary antibody with the appropriate non-specific normal mouse and rabbit IgG (Dako, Kyoto, Japan) at the same concentration. As an additional control, the primary antibody was omitted. After incubation with the primary

antibody, the sections were then incubated at RT for 1 h with appropriate secondary antibodies, Alexa Fluor 488 conjugated anti-mouse and rabbit IgG antibody (Molecular Probes Inc., Eugene, OR, USA). After several washings with PBS, the sections were coverslipped using anti-fading mounting medium containing propidium iodide (Vectashield; Vector, Burlingame, CA, USA) and examined by confocal microscopy (Olympus Fluoview, Tokyo, Japan).

2.4. Electron microscopy

TT-FDAM was examined by scanning electron microscopy (SEM) and transmission electron microscopy (TEM). AM without epithelium and FDAM were also examined for comparison. Specimens were fixed in 2.5% glutaraldehyde in 0.1 M PBS, washed three times for 15 min in PBS, and post-fixed for 2 h in 2% aqueous osmium tetroxide. They were washed three more times in PBS before being passed through a graded ethanol series. For SEM preparation, specimens were transferred to hexamethyldisilazane (TAAB Laboratories Equipment Ltd., UK) for 10 min and allowed to air-dry. When dry, specimens were mounted on aluminum stubs and sputter-coated with gold before examination in a digital scanning electron microscope (JEOL JSM 5600; JEOL Ltd., Tokyo, Japan). For TEM preparation, the specimens were embedded in Agar 100-epoxy resin (Agar Scientific, UK). Ultrathin (70 nm) sections were collected on copper grids and stained for 1 h each with uranyl acetate and 1% phosphotungstic acid, then for 20 min with Reynold's lead citrate prior to examination on a transmission electron microscope (JEOL JEM 1010; JEOL Ltd.).

2.5. Adhesion of rabbit corneal epithelial cells to the AM

To evaluate the cell adhesion properties of each different AM matrix, a single cell suspension of rabbit corneal epithelial cells was seeded onto the AM without epithelium, FDAM, and TT-FDAM in an incubator at 37 °C for two different lengths of time: 60 min and overnight. Briefly, rabbit corneal epithelial cells including the limbal region were incubated at 37 °C for 1 h with 1.2 IU dispase and then trypsinized at 37 °C for 30 min. The resultant single cell suspension of corneal epithelial cells was then seeded onto each AM matrix spread on the bottom of culture inserts (5×10^4 cells/six well culture insert, $N = 5$). After incubation, non-adherent cells were washed with the culture medium (defined keratinocyte growth medium (ArBlast Co., Ltd., Kobe, Japan) supplemented with 5% FBS) and then adherent cells were trypsinized and the cell number was then counted. In our series, we confirmed macroscopically and histologically that no cells remained attached to the three different types of AM.

2.6. 3D culture of rabbit corneal epithelial cells on TT-FDAM

We cultured rabbit corneal epithelial cells using a previously reported system with some modifications [9]. Briefly, confluent 3T3 fibroblasts were incubated with 4 μg/ml of mitomycin C (MMC) for 2 h at 37 °C under 5% CO₂ to inactivate proliferation. They were then rinsed with PBS, trypsinized, and plated onto plastic dishes at a density of 2×10^4 cells/cm². The TT-FDAM was spread, epithelial-basement-membrane side up, on the bottom of culture inserts (Corning Inc., NY, USA); these inserts were then placed in plastic dishes containing treated 3T3 fibroblasts without direct cell–cell contact. Rabbit corneal epithelial cells including the limbal region were incubated at 37 °C for 1 h with 1.2 IU dispase and then trypsinized at 37 °C for 30 min. The resultant cell suspension of corneal epithelial cells was then seeded onto TT-FDAM spread on the bottom of culture inserts and co-cultured with MMC-inactivated 3T3 fibroblasts without direct cell–cell contact. The culture was submerged in medium (defined keratinocyte growth medium (ArBlast Co., Ltd., Kobe, Japan) supplemented with 5% FBS) for 2 weeks and then exposed to air by lowering the medium level (airlifting) for the final day; the medium was changed daily.

2.7. Biocompatibility of TT-FDAM in vivo

Animals examined in this study were treated in accordance with the ARVO Statement on the Use of Animals in Ophthalmic and Vision Research and with the experimental procedure approved by the Committee for Animal Research at Kyoto Prefectural University of Medicine.

To investigate the compatibility of TT-FDAM with corneal tissue, we transplanted it into the intracorneal stroma ($N = 3$). This was carried out by marking the rabbit cornea 3.0 mm inside the limbus, after which a semilayer incision of the corneal stroma was performed using a micro-knife and a spatula. The TT-FDAM (4 × 4 mm) was then inserted into the intrastromal layer (Supplementary data, Fig. 1). One suture of 10–0 nylon was placed around the corneal wound. Corneal transparency and neovascularization were assessed by slit-lamp microscopy. The transplanted cornea (1 month after transplantation) was stained with hematoxylin and eosin (HE).

To further investigate the biocompatibility of TT-FDAM with the ocular surface, we transplanted it onto the bare sclera surface of a rabbit ($N = 3$). FDAM was also examined for comparison. The transplantation of both TT-FDAM and FDAM was carried out by the following method: first, we removed the rabbit conjunctiva (15 × 10 mm) with surgical scissors. The remaining severed edge of the conjunctiva was secured onto the sclera with 10–0 nylon, and after wiping the scleral surface with a micro-sponge the TT-FDAM and FDAM were then simply put on the sclera

Table 1
Primary antibodies and source

| Antibodies | Category | Dilution | Source |
|---------------------|-------------------|----------|-----------------|
| Collagen 1 | Rabbit polyclonal | X300 | LSL, Japan |
| Collagen 3 | Rabbit polyclonal | X300 | LSL, Japan |
| Collagen 4 | Rabbit polyclonal | X300 | LSL, Japan |
| Collagen 5 | Rabbit polyclonal | X300 | LSL, Japan |
| Collagen 7 | Mouse monoclonal | X100 | Chemicon, USA |
| Fibronectin | Mouse monoclonal | X100 | Novo Castra, UK |
| Laminin 5 | Mouse monoclonal | X100 | Chemicon |
| Keratin 1 | Mouse monoclonal | X20 | Novo Castra |
| Keratin 3 | Mouse monoclonal | X100 | Progen, Germany |
| Keratin 4 | Mouse monoclonal | X200 | Novo Castra |
| Keratin 10 | Mouse monoclonal | X50 | Novo Castra |
| Keratin 13 | Mouse monoclonal | X200 | Novo Castra |
| Muc5ac | Mouse monoclonal | X200 | Zymed, USA |
| CD4 | Mouse monoclonal | X50 | Dako, Japan |
| CD8 | Mouse monoclonal | X50 | Dako, Japan |
| CD68 | Mouse monoclonal | X50 | Dako, Japan |
| Neutrophil elastase | Mouse monoclonal | X50 | Dako, Japan |

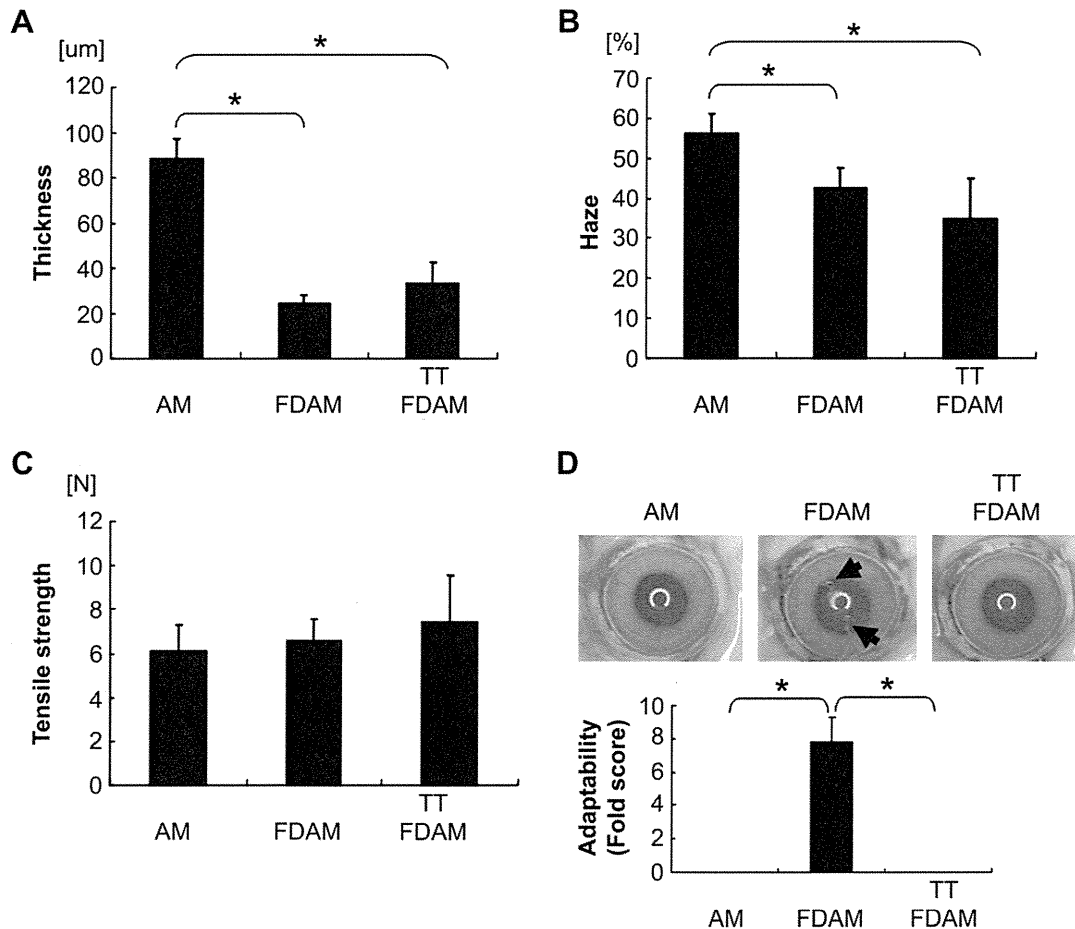


Fig. 1. The graphs show the results of thickness (A), haze (B), tensile strength (C), and adaptability (D) of AM, FDAM, and TT-FDAM, respectively. The thickness of FDAM and TT-FDAM was significantly reduced as compared to native AM (A: *t*-test, $*p < 0.01$). The haze of FDAM and TT-FDAM tended to improve as compared to AM (B: *t*-test, $*p < 0.01$). There were no statistically significant differences in physical tensile strength between AM, FDAM, and TT-FDAM (C: *t*-test, $p > 0.05$). TT-FDAM was smoother and more adaptable than FDAM (D: Mann–Whitney *U*-test, $*p < 0.01$). TT-FDAM was almost identical to native AM.

surface with the epithelial-basement-membrane side facing up. At 4 weeks after transplantation, we examined the epithelialization and hyperemia of the surgical area by slit-lamp microscopy ($N = 3$).

2.8. Statistical analysis

For statistical assessment of the physical characteristics of AM, five different samples were analyzed by Student *t*-test or Mann–Whitney *U*-test. For statistical assessment of adherent cell ratios, five different samples were also analyzed by Student *t*-test.

3. Results

3.1. Appearance and morphological features of TT-FDAM

Visually, FDAM and TT-FDAM were so similar to each other in the dry condition that it was macroscopically difficult to distinguish any difference between the two. The FDAM and TT-FDAM were both wafer-like in appearance, very light and thin, and easy to handle and suture without tearing. Moreover, they both became smooth and flexible upon hydration, however, the TT-FDAM was smoother and more flexible than FDAM in the wet condition (Supplementary data, Movie 1). The results of the bacteriology tests of FDAM and TT-FDAM were all negative in our series.

3.2. Physical characteristics of TT-FDAM

The surface-scanning laser confocal displacement meter showed that the thickness of the AM, FDAM, and TT-FDAM was

88.48 ± 8.81 , 24.24 ± 3.89 , and 33.09 ± 9.32 μm (standard deviations (SD)), respectively, indicating that the freeze-drying process markedly reduced the thickness of the native AM (Fig. 1A, *t*-test, $p < 0.01$). The turbidimeter showed that the haze of the AM, FDAM, and TT-FDAM was 56.18 ± 5.00 , 42.36 ± 5.22 , and 34.75 ± 10.24 (SD), respectively, suggesting that the freeze-drying process decreased the haze of the AM (Fig. 1B, *t*-test, $p < 0.01$). The SS tests were performed on 10×30 mm samples to determine the maximum tear resistance of all membranes. Under wet conditions, AM, FDAM, and TT-FDAM showed a tearing strength of 6.12 ± 1.17 , 6.59 ± 0.97 , and 7.39 ± 2.18 gf (SD), respectively (Fig. 1C). There were no statistically significant differences in the physical tensile strength among AM, FDAM, and TT-FDAM (Fig. 1C, *t*-test, $p > 0.05$). Adaptability assay indicated that there was no AM fold when both AM and TT-FDAM were placed on the cornea. In contrast, there were some AM folds (7.8 ± 1.48 , SD) when FDAM was placed on the cornea (Fig. 1D, Mann–Whitney *U*-test, $p < 0.01$). These results clearly indicated that TT-FDAM has better adaptability than FDAM and is almost identical to native AM.

3.3. Immunofluorescence of extracellular matrix molecules

Three individual AM, FDAM, and TT-FDAM samples were examined. The patterns of extracellular matrix molecule expression in the samples were investigated with immunohistochemistry. Negative control sections, incubated with normal mouse and rabbit IgG and without primary antibody, exhibited no discernible specific

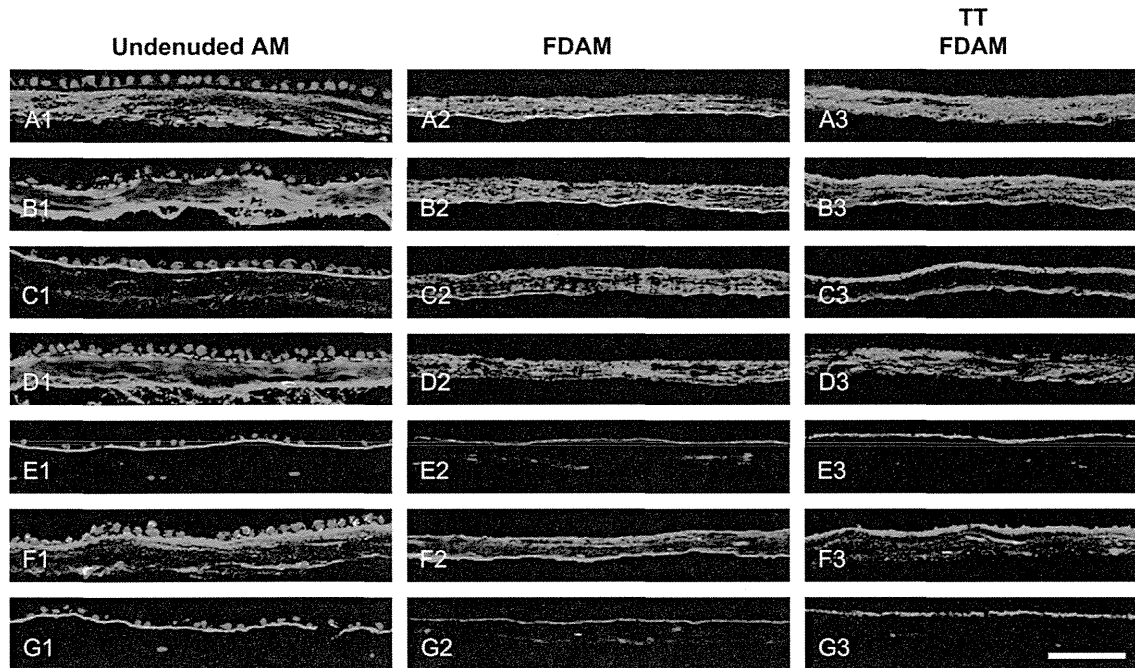


Fig. 2. Representative immunohistochemical staining of collagen 1 (A1–A3), collagen 3 (B1–B3), collagen 4 (C1–C3), collagen 5 (D1–D3), collagen 7 (E1–E3), fibronectin (F1–F3), and laminin 5 (G1–G3) in undenuded AM (A1–G1), FDAM (A2–G2), and TT-FDAM (A3–G3). Collagens 1, 3–5, and fibronectin were expressed throughout the entire AM, FDAM, and TT-FDAM samples. In contrast, collagen 7 and laminin 5 were expressed in the basement membrane side of AM. Nuclei were stained with propidium iodide (red). Scale bar: 100 μm .

immunoreactivity throughout the entire regions. The immunoreactivity observed in each of the three individual samples was compared with these controls. Immunohistochemistry showed the presence of collagens 1, 3–5, and fibronectin throughout the entire AM, FDAM, and TT-FDAM samples (Fig. 2A–D,F). In contrast, collagen 7 and laminin 5 were expressed on the basement membrane side of AM, FDAM, and TT-FDAM (Fig. 2E,G).

3.4. Electron microscopic examination of TT-FDAM

TEM showed the denuded AM surface to have the basal lamina remaining (Fig. 3A). The AM stroma contained widely spaced collagen fibrils and a few scattered cells. SEM showed the AM to

be smooth, but under high magnification minute traces of the denuded cells were visible, giving the surface a slightly textured appearance (Fig. 3D). Next, TEM showed the denuded surface of FDAM to have the basal lamina remaining, but this appeared thinner than in the native AM (Fig. 3B). The FDAM stroma appeared very compressed with the collagen fibrils packed very tightly together. SEM showed the FDAM to be flat and featureless (Fig. 3E). All remaining traces of denuded cells on the FDAM were shrunk down, thus producing a flat featureless surface. Finally, TEM showed the denuded surface of TT-FDAM to have the basal lamina remaining (Fig. 3C). The appearance of the basal lamina was very similar to that of native AM. The stroma contained widely spaced collagen fibrils and a few scattered cells. SEM showed the TT-FDAM

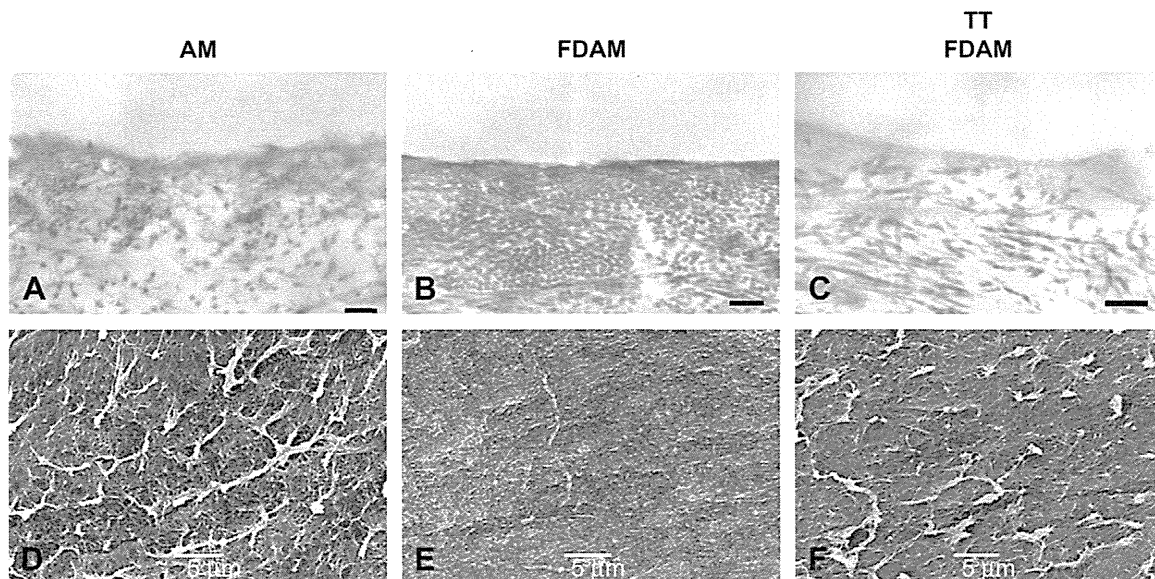


Fig. 3. Representative scanning and transmission electron micrographs of AM, FDAM, and TT-FDAM. The appearance of TT-FDAM (C, F) was more similar to that of AM (A, D) than to FDAM (B, E). In particular, the stroma of AM and TT-FDAM is less compacted than that of FDAM (A–C). Scale bar = 200 nm (A–C) and 5 μm (D–F).

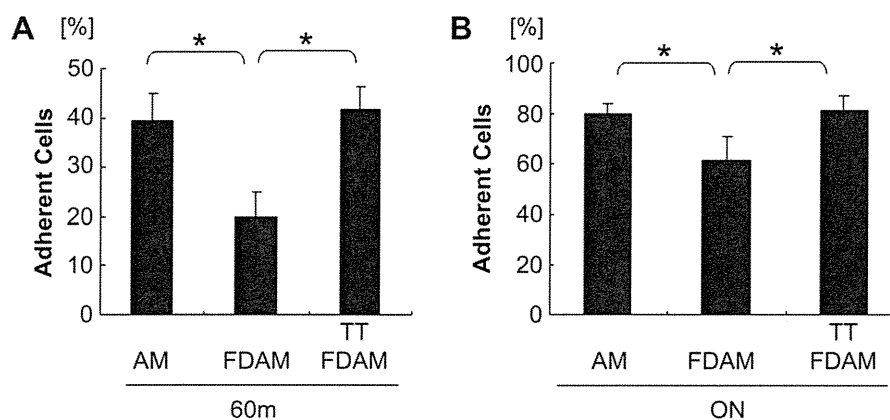


Fig. 4. The adhesion property of AM, FDAM, and TT-FDAM was evaluated by incubating rabbit corneal limbal epithelial cells for different lengths of time including 60 min (A: *t*-test, $*p < 0.01$) and overnight (B: *t*-test, $*p < 0.01$). The adhesion property of TT-FDAM was almost identical to that of native AM.

to be generally smooth, but at high magnification slight traces of the denuded cells remained, giving a textured appearance similar to that observed in native AM (Fig. 3F).

3.5. Adhesion of corneal epithelial cells to AM matrix

The adhesion property of AM, FDAM, and TT-FDAM was evaluated by incubating rabbit corneal epithelial cells for different lengths of time (60 min and overnight). For the 60-min incubation, the percentage of adherent cells on AM, FDAM, and TT-FDAM was 39.3 ± 5.88 , 19.9 ± 5.1 , and 41.7 ± 4.63 (SD), respectively (Fig. 4A). For the overnight incubation, the percentage of adherent cells on AM, FDAM, and TT-FDAM was 79.8 ± 4.11 , 61.4 ± 9.92 , and 81.1 ± 5.93 (SD), respectively (Fig. 4B). These findings indicated that the adhesion property of TT-FDAM was better than that of FDAM, and was almost identical to native AM (Fig. 4, *t*-test, $p < 0.01$).

3.6. Fabrication of cultivated corneal epithelial sheet on TT-FDAM

Corneal epithelial cells began to form colonies on the TT-FDAM within 3 days. After 7 days in culture, a confluent primary culture of corneal epithelial cells had been established that covered the entire TT-FDAM. At 2 weeks, the cultivated corneal epithelial cells showed 4–5 layers of stratification, were well differentiated, and appeared very similar to normal corneal epithelium (Fig. 5A). These sheets showed immunoreactivity for cornea-specific keratin 3, but not epidermal-specific keratin 10 or mucosal-specific keratin 13 (Fig. 5B–D).

3.7. Biocompatibility of TT-FDAM

One month after intracorneal TT-FDAM transplantation, we observed the transplanted rabbit corneal surface by slit-lamp microscopy. The TT-FDAM clarity was markedly improved and there was no neovascularization on the corneal surface (Fig. 6A,B). All of

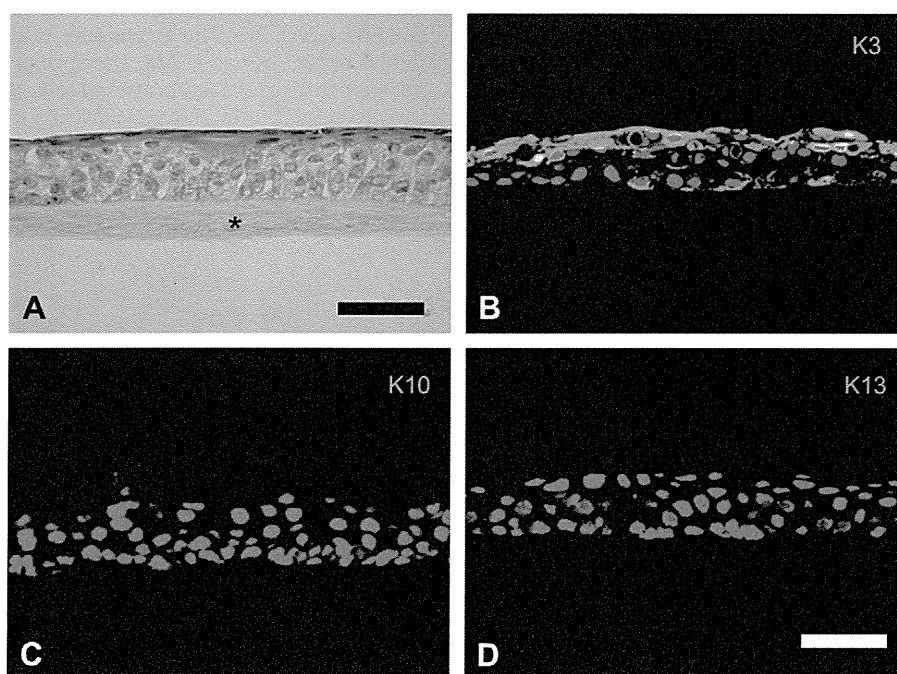


Fig. 5. Light micrograph showing a representative cross-section of the cultivated corneal epithelial cells on TT-FDAM stained with hematoxylin and eosin (A). The cultivated corneal epithelial sheet had 4–5 layers of stratified, well-differentiated cells and appeared very similar to *in vivo* normal corneal epithelium (A). Asterisks indicated TT-FDAM (A). Light micrographs showing immunohistochemical staining for keratin 3 (B), keratin 10 (C), and keratin 13 (D). These sheets showed immunoreactivity for cornea-specific keratin 3, but not epidermal-specific keratin 10 or mucosal-specific keratin 13. Scale bar: 50 μ m (A–D).

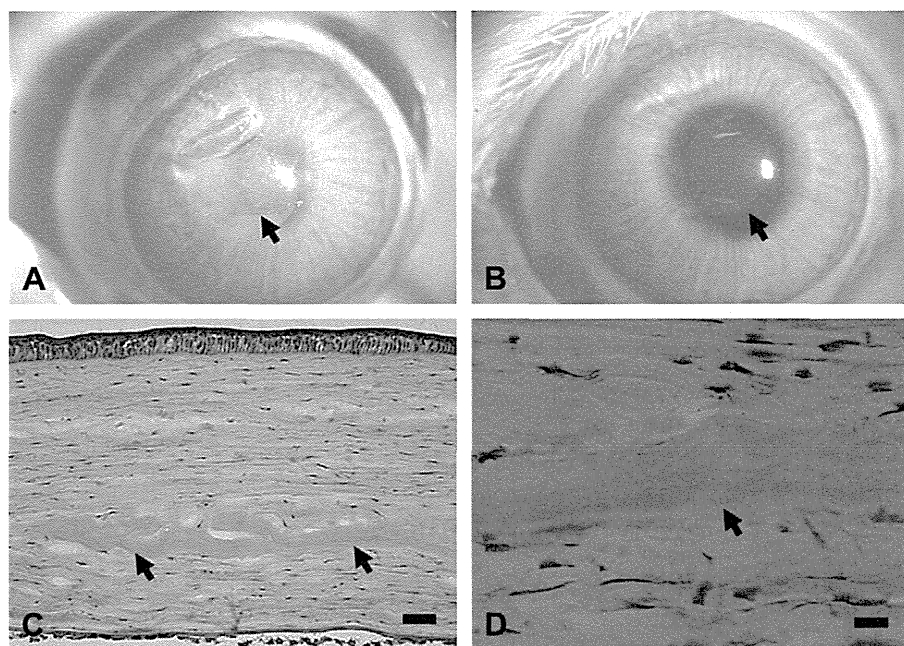


Fig. 6. Representative slit-lamp photographs of one rabbit taken just after intracorneal transplantation (A) and 1 month after transplantation (B) of TT-FDAM. A cross-section of the cornea 1 month after TT-FDAM (C, D). One month after intracorneal TT-FDAM transplantation, there was no evidence of neovascularization or stromal edema on the corneal surface and the clarity of the TT-FDAM was markedly improved (B). The transplanted TT-FDAM adapted well to the host corneal stroma, with no evidence of subepithelial cell infiltration or stromal edema (C, D). Scale bar: 50 μ m (C) and 10 μ m (D).

the transplanted TT-FDAMs adapted well to the host corneal stroma, with no evidence of subepithelial cell infiltration or stromal edema (Fig. 6C,D). Immunohistochemical analysis regarding the inflammatory reaction using several markers (CD4/CD8 (lymphocyte), CD68 (macrophage), neutrophil elastase (neutrophil)) indicated that TT-FDAM did not induce the significant inflammatory reaction *in vivo* (Supplementary data, Fig. 2).

Both TT-FDAM and FDAM were successfully transplanted onto the bare rabbit sclera with sutures as shown in Fig. 7. The secured AMs had been fixed without loss or dislocation for 4 weeks. The grade of epithelialization and hyperemia in the surgical area was

evaluated by slit-lamp microscopy, with and without fluorescein (Fig. 7). Though FDAM transplantation did not epithelialize within 1 week (Fig. 7B), the surface of the TT-FDAM was covered with conjunctival epithelium at 1 week after transplantation (Fig. 7E). In regards to the hyperemia, there was no significant difference between FDAM and TT-FDAM (Fig. 7C,F).

3.8. Characterization of epithelial cells on TT-FDAM

One month after transplantation of FDAM and TT-FDAM onto the bare sclera, we compared the characterization of the migrating

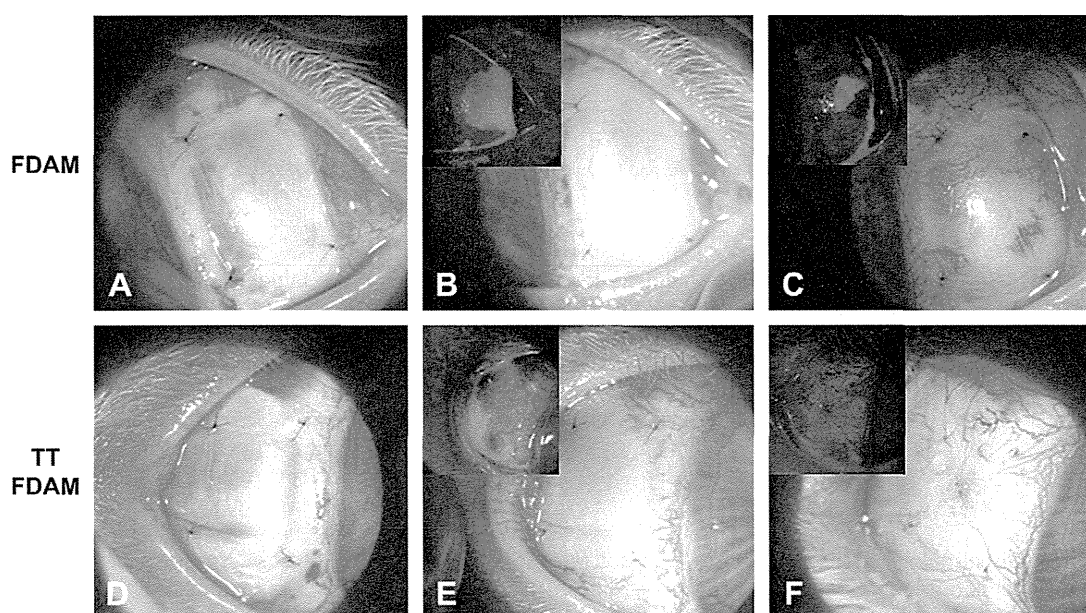


Fig. 7. Representative slit-lamp photographs of rabbit eyes taken just after transplantation (A, D), 7 days after transplantation (B, E), and 1 month after transplantation (C, F) using FDAM (A–C) and TT-FDAM (D–F). Inserts: representative fluorescein images. FDAM transplantation did not epithelialize within 1 week (B), and the surface of the TT-FDAM was covered with conjunctival epithelium at 1 week after transplantation (E). In regards to the hyperemia, there was no significant difference between FDAM and TT-FDAM (C, F).

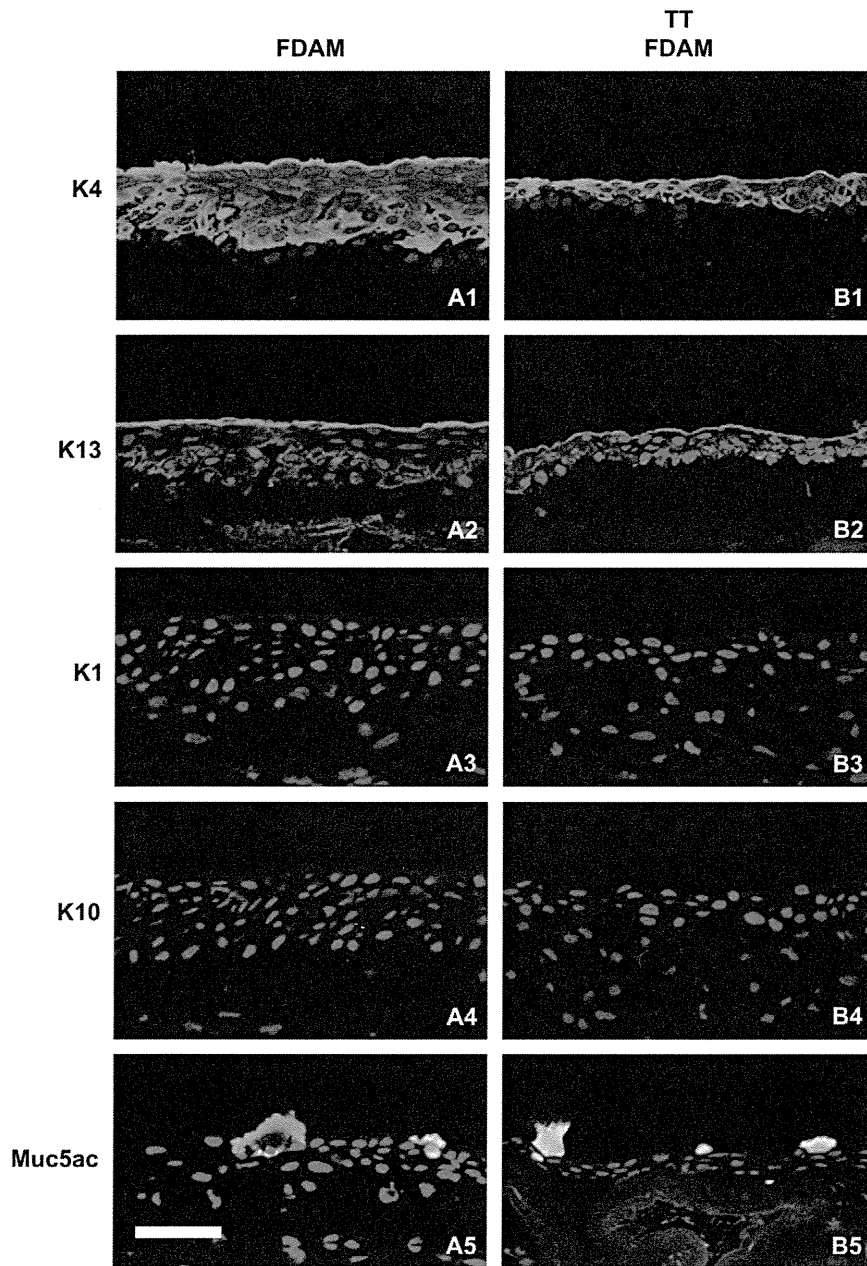


Fig. 8. Representative immunohistochemical staining of K4, K13, K1, K10, and Muc5ac in FDAM (A1–A5) and TT-FDAM (B1–B5). K4, K13, and Muc5ac were expressed at the epithelial cell layer of FDAM (A1, A2, and A5) and TT-FDAM (B1, B2, and B5). In contrast, K1 and K10 were not expressed in any of the FDAM (A3, A4) or TT-FDAM (B3, B4) samples. Scale bar: 50 μ m.

conjunctival epithelial cells on them by immunohistochemistry for keratins 1, 4, 10, 13, and Muc5ac. The staining for keratins 4, 13, and Muc5ac was detected at the epithelial cell layer of both TT-FDAM and FDAM (Fig. 8A1,A2,A5,B1,B2,B5). We were unable to detect any staining for keratins 1 and 10 (Fig. 8A3–A4,B3–B4). These staining patterns were similar to that of *in vivo* normal rabbit conjunctival epithelium [14].

4. Discussion

Currently, most ophthalmologists throughout the world use cryopreserved AM under conditions that are as sterile as possible, however, safe and complete sterilization cannot be guaranteed with present procedures. To overcome this problem, we previously developed the prototype of FDAM by preserving AM in a vacuum-dried state and used gamma-irradiation for sterilization [9]. To

further improve the biological and practical quality of FDAM, we devised a novel manufacturing procedure using a simple trehalose treatment and found that trehalose significantly improved the quality of FDAM. To the best of our knowledge, this is the first study to present the novel concept of using trehalose-treated biomaterials for ocular surface reconstruction.

Our examinations of the physical properties of AM were of particular interest. From our results, the freeze-drying process definitely reduced the thickness of AM, however, SS tests disclosed no significant differences in the mechanical properties of AM, FDAM, or TT-FDAM. Most interestingly, the adaptability of TT-FDAM is markedly improved as compared to FDAM, and it is almost identical to native AM. These findings clearly suggest that the physical properties of TT-FDAM are superior to those of FDAM, and that it has an excellent capacity for wider clinical applications in a variety of research fields.

We thus used several methods to determine the physical properties of TT-FDAM, however, we think that these methods are not accurate enough and more appropriate methods should be selected to determine its exact physical property. For example, haze was measured by turbidimeter, but if a spectroradiometer had been used to determine the coefficients of scattering, absorption, extinction, and translucence using Kubelka–Munk or another type of algorithm, we could have examined its exact transparency. By using a rheometer, it is possible to determine the elastic or viscoelastic behavior of TT-FDAM, along with the dynamic modulus and other relevant parameters of the material. In addition, the method used in this study for the determination of TT-FDAM's adaptability was a subjective method. Therefore, although we were extremely careful with regards to the interpretation of our results, we feel that further investigations using these types of assay are needed to clarify these points.

We previously reported that the organization of the extracellular matrix molecules plays a crucial role in the physical and biological properties of AM. In this study, we examined various kinds of molecular organization and found that collagens 1, 3–5, and fibronectin are expressed throughout the entire TT-FDAM, whereas collagen 7 and laminin 5 are observed in its basement membrane side. These results are almost identical to those of AM and FDAM [9]. Moreover, our electron microscopy results for AM, FDAM, and TT-FDAM showed that the detailed morphological appearance of the TT-FDAM is more similar to that of AM than to FDAM. Even though the expression pattern of basement membrane components and morphological appearance in the three AM types were somehow contradictory, we presume that all AMs examined in this study have the original basement membrane components yet their detailed morphology may change during the freeze-drying process without trehalose treatment. Thus, these physical, immunohistochemical, and morphological examinations confirmed that the simple trehalose treatment worked well for protecting the AM matrix from the process of freeze-drying and irradiation, and well maintained the physical or biological properties of the AM.

To use TT-FDAM as a biomaterial, it is important to examine its biocompatibility. Since trehalose is a kind of sugar, it may induce an inflammatory reaction *in vivo* and may compromise the anti-inflammatory property of AM. Therefore, we examined its biocompatibility by intracorneal transplantation. All transplanted TT-FDAMs examined in this study adapted well to the host corneal stroma, with no evidence of subepithelial cell infiltration, stromal edema, or neovascularization. Nor was there any evidence of infection or rejection on the corneal surface. Our immunohistochemical analysis regarding the inflammatory reaction using several markers indicated that TT-FDAM did not induce the significant inflammatory reaction *in vivo*. We think that trehalose is a chemically inactive and non-permeating agent, which explains why the residual trehalose in TT-FDAM was minimal, affected the surrounding tissues less, and immediately disappeared after transplantation. To further confirm these results, we also examined the biocompatibility by scleral-surface transplantation, and found that TT-FDAM-transplanted eyes showed an almost identical course to FDAM-sutured eyes. Even though our biocompatibility assay was only a 1-month examination, further long-term follow-up studies are needed to confirm their exact biocompatibility.

When TT-FDAM is used for clinical applications, what is of key importance is that it has little influence on the surrounding tissues, especially on migrating conjunctival epithelial cells. We examined the expression of CK1, CK4, CK10, and CK13 in the transplanted TT-FDAM covered with conjunctival epithelium. The epithelium covering expressed the mucosal-specific K4 and K13, and did not express keratinized-marker K1 or K10, indicating that TT-FDAM does not affect the differentiation of the migrating conjunctival epithelium. These results are consistent with the previous report

regarding AM and FDAM [9]. From these results, we are confident that the TT-FDAM we produced shows reasonable biocompatibility with ocular surface tissues.

Recently, AM has been widely used as a substrate for cultivating corneal, conjunctival, and oral mucosal epithelium [17,18]. Therefore, we first examined if TT-FDAM is a suitable substrate for culturing epithelial cells. Adherent cells assay indicated that the cell adhesion property of TT-FDAM was better than that of FDAM, and almost identical to that of AM. Moreover, the cultivated corneal epithelial cells on TT-FDAM showed 4–5 layers of stratification, were well differentiated, and demonstrated immunoreactivity for cornea-specific keratin 3, but not keratins 10 and 13. These findings indicated that TT-FDAM supported normal differentiation of the cells and consequently is an ideal substrate for culturing epithelial cells.

Thus, trehalose has a variety of beneficial effects, and therefore it has been clinically applied in other biological fields for human application. For example, Chen et al. reported that trehalose-containing organ preservation solution is useful for clinical lung transplantation [19]. Moreover, Matsuo et al. reported that trehalose solution was an effective and safe eye drop for the treatment of moderate to severe dry-eye syndrome in their group of patients [20]. Even though trehalose is a natural sugar and is a very safe material, it should be used carefully because sugar may cause the growth of bacteria and mold, etc. In addition, because of the current technical difficulties, we could not fully examine the longevity of trehalose in TT-FDAM. Further investigation into this subject using special procedures and instruments (e.g. special gas chromatography, Fourier-transform infrared analysis, etc.) is needed to clarify these points.

5. Conclusions

In conclusion, our study is the first to demonstrate the usefulness of TT-FDAM for ocular surface reconstruction on the basis of several experiments evaluating physical, morphological, and biological properties. We have shown that compared to FDAM, the TT-FDAM we produced more greatly retains the characteristics of native AM. On the basis of these results, we are in the process of using this biomaterial for ocular surface reconstruction in patients with severe ocular surface diseases and are carefully evaluating the long-term clinical usefulness of TT-FDAM.

Acknowledgements

We thank Mr. J. Bush for editing our manuscript, and Ms. Saito, Horikiri, and Mano for assisting the experimental procedures. This study was supported in part by Grants-in-Aid for Scientific Research from the Japanese Ministry of Health, Labor and Welfare (H16-Saisei-007), and the Japanese Ministry of Education, Culture, Sports, Science and Technology (Kobe Translational Research Cluster), a research grant from the Kyoto Foundation for the Promotion of Medical Science, the Intramural Research Fund of Kyoto Prefectural University of Medicine, and BBSRC in the UK.

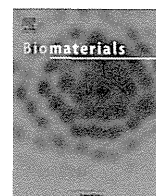
Appendix. Supplementary data

Supplementary data associated with this article can be found, in the online version, at doi:10.1016/j.biomaterials.2008.05.023.

References

- [1] Trelford JD, Trelford-Sauder M. The amnion in surgery, past and present. *Am J Obstet Gynecol* 1979;134(7):833–45.
- [2] Dua HS, Gomes JA, King AJ, Maharajan VS. The amniotic membrane in ophthalmology. *Surv Ophthalmol* 2004;49(1):51–77.

- [3] Kim JS, Kim JC, Na BK, Jeong JM, Song CY. Amniotic membrane patching promotes healing and inhibits proteinase activity on wound healing following acute corneal alkali burn. *Exp Eye Res* 2000;70(3):329–37.
- [4] Solomon A, Rosenblatt M, Monroy D, Ji Z, Pflugfelder SC, Tseng SC. Suppression of interleukin 1alpha and interleukin 1beta in human limbal epithelial cells cultured on the amniotic membrane stromal matrix. *Br J Ophthalmol* 2001;85(4):444–9.
- [5] Tseng SC, Li DQ, Ma X. Suppression of transforming growth factor-beta isoforms, TGF-beta receptor type II, and myofibroblast differentiation in cultured human corneal and limbal fibroblasts by amniotic membrane matrix. *J Cell Physiol* 1999;179(3):325–35.
- [6] Talmi YP, Sigler L, Inge E, Finkelstein Y, Zohar Y. Antibacterial properties of human amniotic membranes. *Placenta* 1991;12(3):285–8.
- [7] Hao Y, Ma DH, Hwang DG, Kim WS, Zhang F. Identification of antiangiogenic and antiinflammatory proteins in human amniotic membrane. *Cornea* 2000;19(3):348–52.
- [8] Akle CA, Adinolfi M, Welsh KI, Leibowitz S, McColl I. Immunogenicity of human amniotic epithelial cells after transplantation into volunteers. *Lancet* 1981;2(8254):1003–5.
- [9] Nakamura T, Yoshitani M, Rigby H, Fullwood NJ, Ito W, Inatomi T, et al. Sterilized, freeze-dried amniotic membrane: a useful substrate for ocular surface reconstruction. *Invest Ophthalmol Vis Sci* 2004;45(1):93–9.
- [10] Nakamura T, Inatomi T, Sekiyama E, Ang LPK, Yokoi N, Kinoshita S. Novel clinical application of sterilized, freeze-dried amniotic membrane to treat patients with pterygium. *Acta Ophthalmol Scand* 2006;84(3):401–5.
- [11] Sekiyama E, Nakamura T, Kurihara E, Cooper LJ, Fullwood NJ, Takaoka M, et al. Novel sutureless transplantation of bioadhesive-coated freeze-dried amniotic membrane for ocular surface reconstruction. *Invest Ophthalmol Vis Sci* 2007;48:1528–34.
- [12] Guo N, Puhlev I, Brown DR, Mansbridge J, Levine F. Trehalose expression confers desiccation tolerance on human cells. *Nat Biotechnol* 2000;18(2):168–71.
- [13] Crowe JH, Crowe LM, Oliver AE, Tsvetkova N, Wolkers W, Tablin F. The trehalose myth revisited: introduction to a symposium on stabilization of cells in the dry state. *Cryobiology* 2001;43(2):89–105.
- [14] Nakamura T, Endo K-I, Cooper LJ, Fullwood NJ, Tanifuji N, Tsuzuki M, et al. The successful culture and autologous transplantation of rabbit oral mucosal epithelial cells on amniotic membrane. *Invest Ophthalmol Vis Sci* 2003;44(1):106–16.
- [15] Nakamura T, Endo K, Kinoshita S. Identification of human oral keratinocyte stem/progenitor cells by neurotrophin receptor p75 and the role of neurotrophin/p75 signaling. *Stem Cells* 2007;25(3):628–38.
- [16] Nakamura T, Ohtsuka T, Sekiyama E, Cooper LJ, Kokubu H, Fullwood NJ, et al. Hes1 regulates corneal development and the function of corneal epithelial stem/progenitor cells. *Stem Cells* 2008;26(5):1265–74.
- [17] Tsai RJ-F, Li L-M, Chen J-K. Reconstruction of damaged corneas by transplantation of autologous limbal epithelial cells. *N Engl J Med* 2000;343(2):86–93.
- [18] Koizumi N, Inatomi T, Suzuki T, Sotozono C, Kinoshita S. Cultivated corneal epithelial stem cell transplantation in ocular surface disorders. *Ophthalmology* 2001;108(9):1569–74.
- [19] Chen F, Fukuse T, Hasegawa S, Bando T, Hanaoka N, Kawashima M, et al. Effective application of ET-Kyoto solution for clinical lung transplantation. *Transplant Proc* 2004;36(9):2812–5.
- [20] Matsuo T, Tsuchida Y, Morimoto N. Trehalose eye drops in the treatment of dry eye syndrome. *Ophthalmology* 2002;109(11):2024–9.



Sutureless amniotic membrane transplantation for ocular surface reconstruction with a chemically defined bioadhesive

Maho Takaoka^a, Takahiro Nakamura^{a,b,*}, Hajime Sugai^c, Adam J. Bentley^d, Naoki Nakajima^c, Nigel J. Fullwood^d, Norihiko Yokoi^a, Suong-Hyu Hyon^c, Shigeru Kinoshita^a

^a Department of Ophthalmology, Graduate School of Medicine, Kyoto Prefectural University of Medicine, Kyoto 602-0841, Japan

^b Research Center for Regenerative Medicine, Doshisha University, Kyoto 602-8580, Japan

^c Institute for Frontier Medical Sciences, Kyoto University, Kyoto 606-8501, Japan

^d Biomedical Sciences Unit, Biological Sciences, Lancaster University, Lancaster LA1 4YW, UK

ARTICLE INFO

Article history:

Received 19 February 2008

Accepted 18 March 2008

Available online 15 April 2008

Keywords:

Ophthalmology
Transplantation
Sutureless
Ocular surface
Bioadhesive
Biocompatibility

ABSTRACT

The purpose of this study was to evaluate the efficiency and safety of a sutureless amniotic membrane transplantation (AMT) for ocular surface reconstruction with a chemically defined bioadhesive (CDB). The CDB was synthesized from aldehyded polysaccharides and ϵ -poly(L-lysine), two kinds of medical and food additives, as starting materials. Biocompatibility assay indicated that the CDB showed excellent biocompatibility with *in vitro* and *in vivo* ocular surface tissues and most of the CDB was histologically degraded within 4 weeks. Sutureless AMT using the CDB was safely and successfully performed onto a rabbit scleral surface. Transplanted amniotic membrane (AM) evaluated by histological, electron microscopic- and immunohistochemical examination indicated that the CDB did not affect normal differentiation of the cells or the integrity of the surrounding tissue. Thus, this newly developed CDB was found to be very useful for sutureless AMT for ocular surface reconstruction, without considering the risk of infection. It has the ability to fix AM to the ocular surface for a long time-period without additional inflammation, scarring, or damage to the surrounding tissues.

© 2008 Elsevier Ltd. All rights reserved.

1. Introduction

Human amniotic membrane (AM) has been shown to possess various kinds of biological effects such as anti-inflammatory [1,2], antifibroblastic [3], anti-microbial [4], and anti-angiogenic properties [5], and promote epithelialization by facilitating the migration of epithelial cells [6], reinforcing adhesion of basal epithelial cells, and promoting epithelial differentiation [7]. It also produces growth factors that promote epithelial cell growth [8]. Due to these desirable properties, AM has been used as surgical material in a wide variety of operations. Since Kim and Tseng achieved successful corneal re-epithelialization in chemical burns by amniotic membrane transplantation (AMT) in 1995 [9], AM has been widely used in eyes with ocular surface diseases such as persistent corneal epithelial defects [10,11], pterygium [12], symblepharon [13,14], and stem cell deficiency [9,13,15–18].

AM is usually sutured onto the ocular surface using 10-0 nylon sutures to fix [19]. Although the suturing method makes for

a secure attachment, it inflicts trauma to the ocular surface. Moreover, a prolonged operative time and technical skill are needed for effective suture placement. Sutures can not only cause postoperative pain and discomfort which is a significant problem for patients [20], but can also be associated with suture-related complications such as suture abscesses [21,22], granuloma formation [23], and tissue necrosis [24]. To solve these problems, sutureless techniques have been applied for various kinds of operations on the ocular surface including conjunctival closure after surgery [25,26], pterygium surgery [20,27,28], corneal stem cell transplantation [29,30], lamellar keratoplasty [31], and conjunctivochalasis [32].

Recently, we developed a sutureless AMT using bioadhesive-coated freeze-dried AM for ocular surface reconstruction [33]. This AM is based on our previous report regarding sterilized, freeze-dried AM [34]. Being coated by a minimum dose of fibrin glue, bioadhesive-coated freeze-dried AM can be readily used after opening the package. It can be kept sterilized at room temperature (RT) for long periods without deterioration so that it can easily be stored, transported, and used. This 'ready-to-use' AM has enabled AMT to be easily performed in every hospital in the world.

Although these newly developed sutureless methods using fibrin glue achieved successful outcomes, safety and logistical problems still remain. Some viruses, such as parvovirus B19 (HPV

* Corresponding author. Department of Ophthalmology, Kyoto Prefectural University of Medicine, Kawaramachi Hirokoji, Kamigyo-ku, Kyoto 602-0841, Japan. Tel.: +81 75 251 5578; fax: +81 75 251 5663.

E-mail address: tnakamur@ophth.kpu-m.ac.jp (T. Nakamura).

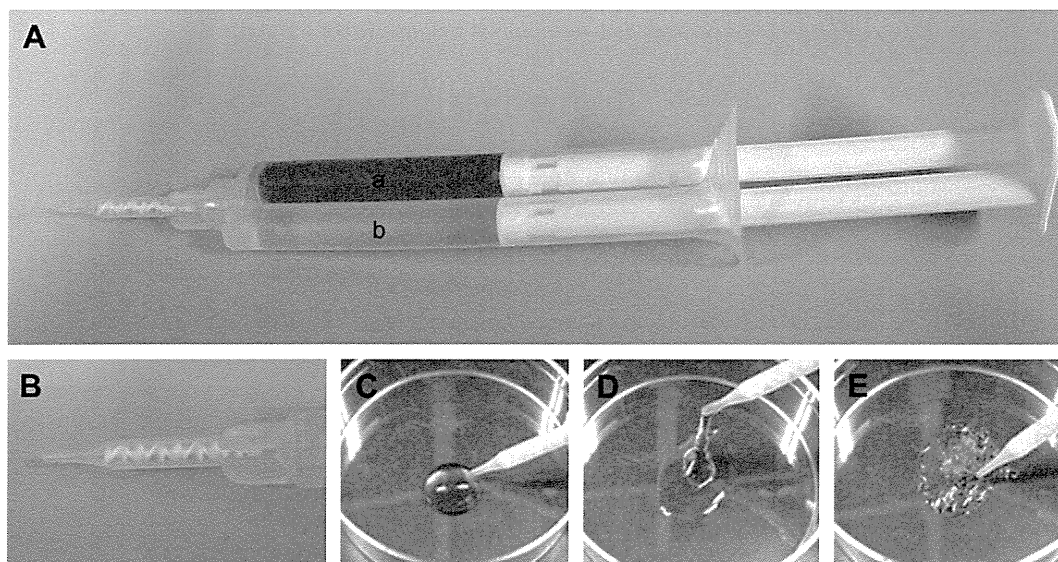


Fig. 1. (A) This glue prepared with syringe-like container with two cylinders (a, b); one cylinder (a) is filled with 2 ml of 14 w/w% aldehyded dextran solution with aldehyde introduced ratio of 0.43 per sugar unit, and the other (b) with 2 ml of 7 w/w% ϵ -poly(L-lysine) solution containing 2.1% w/w% acetic anhydride. The container has special mixing tip which can mix two solutions each other by equal volume as passing through it (B). The mixed adhesive is gradually gelatinized (C–E). The tip is disposable because the adhesive had been gelatinized in the tip before next application.

B19) are particularly difficult to totally remove or inactivate, and human infection has been reported after the use of fibrin glue that had been prepared in house from pooled plasma [35]. Moreover, in thoracic surgery, epidemiological evidence suggests that more than 20% of uninfected people were subsequently infected with HPV B19 by use of commercially available fibrin sealant during the procedure [36]. In addition, there is a potential for the transmission of prions originating even from commercially available human plasma [37]. Although the risks of both diseases are extremely low, patients should be informed before surgery. Some other tissue adhesives using collagen or gelatin of animal sources have been previously developed and experimentally evaluated, but like with fibrin glue, the risks of infection have still remained. If non-biologic and chemically defined bioadhesives can be successfully applied, it would prove ideal for safe and simple ocular surface reconstruction.

In this report, we present our newly developed CDB for sutureless AM transplantation. It was made from antibiotic food additives and characterized by its self-degradability, low toxicity, and stronger bonding property. To the best of our knowledge, there have been no reports investigating ocular surface reconstruction using safe and effective CDB.

2. Materials and methods

2.1. Preparation of CDB

The mechanism of CDB gelation is based on Schiff base formation between oxidized and aldehyded polysaccharides and ϵ -poly(L-lysine), two kinds of antibacterial additives for medicine or food [38]. CDB is prepared with a syringe-like container with two cylinders (Fig. 1A). One cylinder is filled with 2 ml of 14% w/w aldehyded dextran solution (molecular weight: 75K Da) with aldehyde introduced ratio of 0.43 per sugar unit, and the other with 2 ml of 7% w/w ϵ -poly(L-lysine) solution (molecular weight: 4K Da) containing 2.1% w/w acetic anhydride. CDB was

used after filtration sterilization of both solutions using a syringe filter with 0.2 μ m pore size. When the end of the syringe is pushed, the two solutions are mixed together in equal volumes as they pass through the tip (Fig. 1B) and then gradually gelatinize (Fig. 1C–E). Gel formation time, which can be altered by aldehyde introduction in dextran, was approximately 31 seconds at the temperature of 37 °C, counted by the same method as in the previous report [38]. Degradation speed can also be altered by acetic anhydride concentration in ϵ -poly(L-lysine). The CDB in this report was self-degradable within 4 days at the temperature of 37 °C *in vitro*.

2.2. Preparation of AM

AMs were prepared according to our previously reported method [39]. Briefly, after obtaining proper informed consent in accordance with the tenets of the Declaration of Helsinki, and with approval by the Institutional Review Board of Kyoto Prefectural University of Medicine, human AM was obtained under a sterile condition from seronegative donors after an elective caesarean section. The AM was washed with sterile phosphate buffered saline (PBS) (Nissui, Tokyo, Japan) containing antibiotics and antimycotics. The chorion was peeled off manually and epithelial cells were removed by incubation with 0.02% ethylene diamine tetra-acetic acid (EDTA) (Nacalai, Kyoto, Japan) at 37 °C for 2 h. Denuded AM was cut into approximately 4 × 4 cm pieces, and cryopreserved at –80 °C in a sterile vial containing Dulbecco's modified Eagle medium and glycerol in a volume ratio of 1:1. Before use, the AM was thawed by warming the vial to RT.

2.3. Examination of biocompatibility of CDB

Before using the CDB in this assay, we have already investigated each cytotoxicity test of aldehyded dextran and poly(L-lysine) using mouse established cell line L929 [38]. IC50 (sample concentration in culture medium which suppresses the cell viability down to 50%) of them was 6000 and >10,000 μ g/ml, respectively. These values are 1000 times as much as those of formaldehyde and glutaraldehyde (1.7 and 3.9 μ g/ml, respectively), which suggests quite the low toxicity of both components. Because the difficulty in cytotoxic evaluation of hydrogel materials *in vitro*, *in vivo* biocompatibility test of gelation sample was carried out. All experiments in this study were performed in accordance with the Committee for Animal Research at Kyoto Prefectural University of Medicine and according to the ARVO statement on the Use of Animals in Ophthalmic and Vision Research. To investigate the biocompatibility of CDB with the ocular surface, it was injected into the subconjunctival

Table 1
Antibodies and their sources

| Specificity | Immunized | Dilution | Sources | Cat. number |
|----------------|------------|----------|------------|-------------|
| Cytokeratin 1 | Mouse, mAb | 20× | Novocastra | NCL-CK1 |
| Cytokeratin 4 | Mouse, mAb | 200× | Novocastra | NCL-CK4 |
| Cytokeratin 10 | Mouse, mAb | 50× | Novocastra | NCL-CK10 |
| Cytokeratin 13 | Mouse, mAb | 200× | Novocastra | NCL-CK13 |
| MUC5AC | Mouse, mAb | 200× | Zymed | 18-2261 |

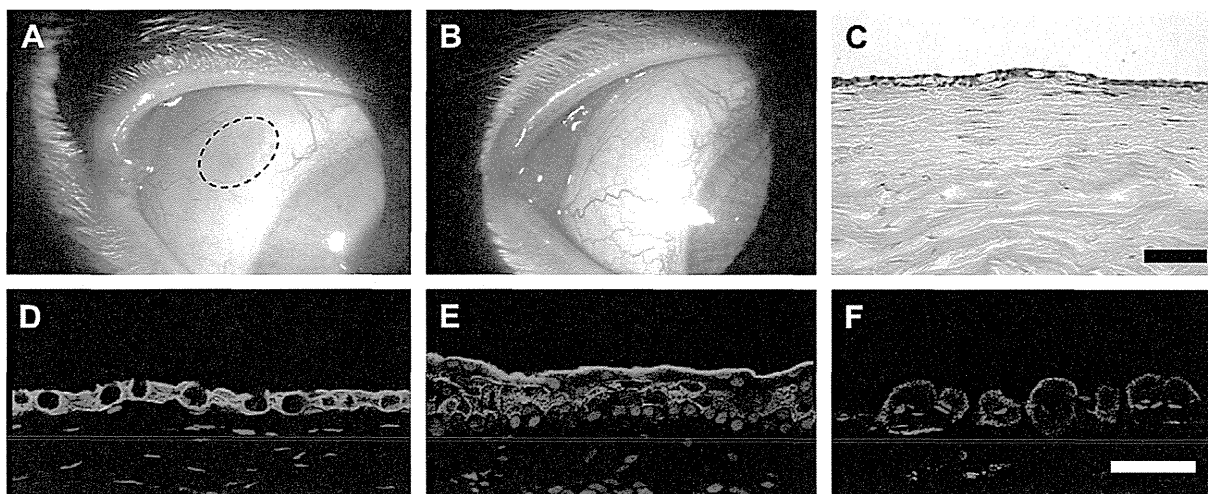


Fig. 2. Representative finding of slit lamp examination immediately (A) and 4 weeks (B) after the subconjunctival injection of the bioadhesive. Injected area could be identified by blue area translucent through conjunctiva (dashed circle). H&E staining (C) and immunohistochemical staining of CK4 (D) and 13 (E), and MUC5AC (F) in injected area revealed that they were similar to normal tissue. Nuclei were stained with propidium iodide (red). Scale bars: 50 μ m.

space of a rabbit eye. A 27-gauge needle was attached at the tip of the syringe and a small amount of CDB (approximately 0.1 ml) was subconjunctivally injected. Four weeks after injection, tissues were removed and cryostat sections were stained with hematoxylin and eosin.

2.4. Sutureless transplantation

To investigate the adherence and biocompatibility of the CDB to the ocular surface, AM was transplanted onto the rabbit sclera using CDB. AMT with sutures and simple recession of the sclera without AMT were also performed as a control.

First, the rabbit conjunctiva (15 \times 10 mm) was removed with surgical scissors and the severed edge of the conjunctiva was secured onto the sclera with 9-0 silk so that the sufficient size of sclera was exposed. For the sutureless AMT, a drop of CDB was put onto the bare sclera from the tip of the syringe, and then the squarely

trimmed AM was transferred into place with the epithelial basement membrane side up. Excess fluid that extruded from the interface was rubbed off with a sponge and approximately 3 min elapsed before the AM was fixed. For the conventional AMT, the AM was secured at the corner of the membrane onto the bare sclera using 10-0 nylon sutures. The operated eye was patched with a topical antibiotic ointment (0.3% ofloxacin), and a topical steroid/antibiotic ointment was applied once daily for a week. Operations were performed on three rabbits for each group.

At 2, 4, 8, and 12 weeks after transplantation, the grade of epithelialization and hyperemia in the surgical area was examined by slit lamp microscopy. The rabbit was euthanized by the phlebotomy of 1 ml pentobarbital sodium, and the tissue was embedded in OCT compound (Tissue-Tek[®]; Miles Inc., Elkhart, IN, USA) and frozen with liquid nitrogen. Cryostat sections were stained with hematoxylin and eosin. The interface between the sclera and AM was also checked by electron microscopy 1 day after transplantation. To investigate the biological effect of CDB on cells and surrounding tissues, collected tissues were

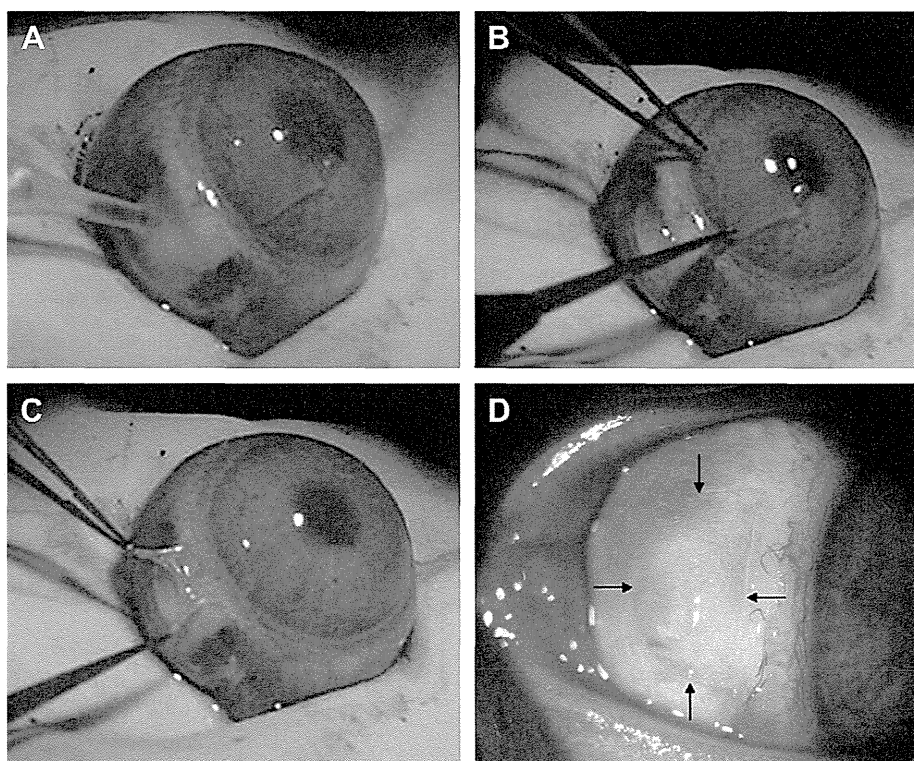


Fig. 3. Representative photos of sutureless AMT. A drop of the bioadhesive was put onto the bare sclera from the tip of the syringe (A), and then the squarely trimmed AM was transferred into the place with the epithelial basement membrane side up (B and C). Excess fluid that extruded from the interface was rubbed off with a sponge and approximately 3 min elapsed before the AM was fixed. Immediately after sutureless AMT, AM was firmly secured on the bare sclera (D).